Wǔhàn sharpbelly bornavirus (genus *Cultervirus*) can infect a wide range of host cells and establishes persistent infection in diverse cypriniform cells

Mirette I. Y. Eshak[1], Angele Breithaupt[2], Birke A. Tews[3], Christine Luttermann[3], Kati Franzke[3], Marion Scheibe[4], Sören Woelke[3], Dennis Rubbenstroth[1], Martin Beer[1] and Florian Pfaff[1,*]

1: Friedrich-Loeffler-Institut, Institute of Diagnostic Virology, Greifswald - Insel Riems, Germany

2: Friedrich-Loeffler-Institut, Department of Experimental Animal Facilities and Biorisk Management, Greifswald - Insel Riems, Germany

3: Friedrich-Loeffler-Institut, Institute of Infectology, Greifswald - Insel Riems, Germany

4: Friedrich-Loeffler-Institut, Institute of Molecular Virology and Cell Biology, Greifswald - Insel Riems, Germany

*Corresponding author: Florian Pfaff

E-mail: florian.pfaff@fli.de

Tel: +49 38351 7 1385

Fax: +49 38351 7 1226

Abstract word count: 249

Importance word count: 148

Main text word count: 8945

Figure count: 8

Reference count: 41

Keywords: *Bornaviridae*, *Cultervirus*, fish, Cypriniformes, metagenomics, infection, persistence

ABSTRACT

Our recent study using *in silico* data mining identified novel culterviruses (*Bornaviridae*) in fish, including a variant of Wǔhàn sharpbelly bornavirus (WhSBV) in grass carp kidney and liver cell lines. Here, metagenomic sequencing of different fish cell lines revealed WhSBV in two additional grass carp swim bladder cell lines, GSB and CiSB. Using these cell lines, we investigated the ability of WhSBV to infect and establish persistent infection in other cell lines from bony fish (Cypriniformes, Chichliformes, Salmoniformes, Centrarchiformes and Spariformes), reptiles (Testudines and Squamata), birds (Galliformes) and mammals (Primates and Rodentia). WhSBV showed efficient replication and a time-dependent increase in viral RNA levels in cypriniform cells, whereas replication was limited, confined to single cells, and lacked a clear time-dependent increase in certain bony fish and reptilian cells. No persistent replication was detected in avian or mammalian cells. *In situ* hybridisation and electron microscopy confirmed the presence of viral RNA and particles in infected fish cells. Transcriptomic sequencing revealed minimal innate immune activation during early stages of infection and antiviral response only at later stages, suggesting that WhSBV establishes persistence by evading early immune recognition. In addition, we identified polycistronic viral mRNAs regulated by specific transcriptional start and termination sites and RNA splicing. Viral proteins were detected, confirming previous *in silico* predictions. These findings provide insights into the potential infectivity, persistence mechanisms and transcriptional strategies of WhSBV. This study validates previous findings from *in silico* data mining, further reinforcing its effectiveness as a powerful tool for discovering hidden viruses.

IMPORTANCE

Understanding the diversity and host range of viruses is crucial for assessing their ecological role, associated diseases and zoonotic potential. However, many newly discovered viruses are characterised using sequence data alone because isolates are often difficult to obtain. Using cell culture models, this study characterises Wǔhàn sharpbelly bornavirus (WhSBV), a member of the genus *Cultervirus*. Here we demonstrate its ability to establish persistent infections in cypriniform fish cell lines, while exhibiting restricted replication in non-cypriniform fish and reptilian hosts. The identification of polycistronic transcription, splicing events and immune evasion mechanisms advances our understanding of the molecular biology of WhSBV and culterviruses in general. By validating *in silico* predictions, this study highlights the power of computational approaches in uncovering viral diversity. As cypriniform fish

include economically important species such as carp, understanding the dynamics of WhSBV host range and infection biology may be crucial for future aquaculture health management.

INTRODUCTION

The family *Bornaviridae*, within the order *Mononegavirales*, contains four genera: *Orthobornavirus*, *Carbovirus*, *Cultervirus*, and *Cartilovirus* (Kuhn et al. 2015; Eshak et al. 2023; Rubbenstroth et al. 2021). The genus *Orthobornavirus* has the broadest known host range, infecting avian, reptilian, and mammalian species (Rubbenstroth et al. 2021). Furthermore, orthobornaviruses include zoonotic viruses, such as Borna disease virus 1 (BoDV-1) and variegated squirrel bornavirus 1 (VSB-1), both of which can cause fatal encephalitis in humans (Niller et al. 2020; Hoffmann et al. 2015). Carboviruses and culterviruses, on the other hand, have only been found in reptiles and fish, respectively, and no zoonotic spillover has been reported (Rubbenstroth et al. 2021; Shi et al. 2018; Eshak et al. 2023; Hyndman et al. 2018). The genus *Cartilovirus* currently only includes the little skate bornavirus (LSBV), which was discovered using public datasets from the Sequence Read Archive (SRA) (Eshak et al. 2023).

Bornavirids possess enveloped virions that enclose a linear, negative-sense, monopartite RNA molecule of approximately 9,000 nucleotides (nt) (Briese et al. 1994; Rubbenstroth et al. 2021). Their genomes encode for at least six open reading frames (ORFs) arranged in the order 3'-N-X/P-M-G-L-5' for orthobornaviruses or 3'-N-X/P-G-M-L-5' for carboviruses and culterviruses. These ORFs encode for six viral proteins; nucleoprotein (N), accessory protein (X), phosphoprotein (P), matrix protein (M), glycoprotein (G), and the large protein (L) which contains a RNA-directed RNA polymerase (RdRP) (Briese et al. 1994; Rubbenstroth et al. 2021). Recently, the largest bornavirid genome, comprising 11,090 nt, was identified for the cartilovirus LSBV. The LSBV genome encodes two additional possible ORFs, viral proteins 1 and 2 (vp1 and -2), and represents a unique genomic architecture 3'-N-vp1-vp2-X/P-G-M-L-5' (Eshak et al. 2023). Studies of BoDV-1 have demonstrated that its RNA and genome are transcribed and replicated in the host cell nucleus, respectively (Briese et al. 1992). In bornavirids, the generation of a diverse array of mRNAs is regulated by differential use of transcription start and termination sites (Schneemann et al. 1994), as well as alternative splicing of polycistronic primary transcripts to increase and control their transcriptional complexity (Schneider et al. 1994; Tomonaga et al. 2000).

Wǔhàn sharpbelly bornavirus (WhSBV, NC_055169; species *Cultervirus hemicultri*), a member of the genus *Cultervirus*, was initially identified by RNA sequencing of the gut, liver,

and gill tissues from a freshwater sharpbelly (*Hemiculter leucisculus* [Basilewsky, 1855], family Xenocyprididae, order Cypriniformes) from China (Shi et al. 2018; Rubbenstroth et al. 2021). Our recent study using *in silico* data mining of publicly available sequencing datasets led to the identification of novel fish culterviruses, including the first complete genome of the Murray-Darling carp bornavirus (MDCBV, BK063521) from a goldfish (*Carassius auratus* [Linnaeus, 1758], family Cyprinidae, order Cypriniformes) tissue pool data set and a WhSBV variant (BK063520) detected in grass carp (*Ctenopharyngodon idella* [Valenciennes, 1844], family Xenocyprididae, order Cypriniformes) CIK (kidney) and L8824 (liver) cell lines (Eshak et al. 2023). The two viruses belong to the same bornavirid species (*Cultervirus hemicultri*) and share 78% nt overall identity. However, current knowledge of these culterviruses remains limited to *in silico* genetic discoveries and bioinformatic predictions, with no virus isolates available for experimental research.

To deepen our understanding of the biology and abundance of culterviruses, we screened 48 fish-derived cell lines for the presence of known or novel culterviruses using metagenomic RNA sequencing. This revealed the presence of WhSBV in two grass carp swim bladder cell lines, GSB (CCLV no. 1441) and CiSB (1542), with genomes nearly identical to the WhSBV variant from the liver and kidney cell lines (BK063520). This study represents the first investigation into the biology of WhSBV and lays the groundwork for future research to further explore culterviruses.

MATERIALS AND METHODS

Nucleic acids extraction and metagenomic sequencing

A total of 48 fish cell lines were provided by the Collection of Cell Lines in Veterinary Medicine (CCLV) (see Supplementary Table S1 for a complete list of cell lines) at the Friedrich-Loeffler-Institut, Riems, Germany. Fresh-frozen cell lines were lysed in 1 ml TRIzol LS reagent (Life Technologies) and shaken vigorously for 10 min at room temperature. After addition of 200 µl chloroform (Carl Roth GmbH & Co. KG) and centrifuging at 13,000 × g, 10 min, 4°C, 200 µl of the upper aqueous phase was used for RNA extraction. Total RNA was extracted using the Agencourt RNAdvance Tissue Kit (Beckman Coulter) with a KingFisher Flex Purification System (Thermo Fisher Scientific) according to the manufacturer's instructions. DNase I digestion (Qiagen) was carried out prior to the final elution to remove genomic DNA residues. The quantity of total RNA was determined using the NanoDrop Lite Spectrophotometer (Thermo Fisher Scientific). Poly(A) RNA was isolated using the Dynabeads mRNA DIRECT Purification Kit (Invitrogen) following the manufacturer's instructions. Fragmentation and strand-specific construction of whole transcriptome libraries was performed using the Collibri Stranded RNA Library Prep Kit for Illumina Systems (Invitrogen). The quality and integrity of the RNA and the final library were verified using the Agilent TapeStation 4150 (Agilent Technologies) with appropriate chips and reagents. The final libraries were quantified using the Qubit dsDNA HS Assay Kit (Invitrogen) in combination with the Qubit 2.0 Fluorometer (Invitrogen). Equimolar amounts of the library were then sequenced using Novaseq 6000 with SP flow cell, 1 x 101 bp (CeGat GmbH) according to the manufacturer's instructions.

Metagenomic analysis

The raw reads obtained from the 48 fish cell lines were trimmed using *TrimGalore!* (v0.6.10) and *cutadapt* (v4.0). The metagenomic pipeline *SqueezeMeta* (v1.6.4) was then used to individually assemble the trimmed reads from each dataset and then sequentially merge them into a single transcriptome ("seqmerge" mode). The assembled and merged transcripts were then filtered for poly(A/T) sequences at their termini using *cutadapt* (v4.0). The filtered transcriptome was then used as input for taxonomic assignment and abundance estimation using *SqueezeMeta* (v1.6.4, database version Sep-3-2023). The results were further analysed using the R (v4.3.1) package "SQMtools" (v1.6.3).

Validation of WhSBV genome termini

Persistently WhSBV-infected GSB and CiSB cell cultures (see Supplementary Table S1) were grown in non-vented T25 tissue culture flasks (Corning, Inc.) in a suitable growth medium supplemented with 10% fetal bovine serum (FBS) to 95-100% confluence. Total RNA was extracted using the TRIzol-chloroform method, followed by purification using the RNeasy Mini Kit (Qiagen) and DNase I digestion prior to elution. The quality and quantity of the RNA were assessed using the Agilent TapeStation 4150 in combination with appropriate chips and reagents, and the NanoDrop Lite spectrophotometer, respectively.

The 5'-Rapid Amplification of cDNA Ends (RACE) kit, version 2.0 (Invitrogen), was used to determine the 3' end of the WhSBV genome. Reverse transcription polymerase chain reaction (RT-PCR) was performed on the extracted RNA using a gene-specific primer WhSBV-945-R (0.4 µM) (see Supplementary Table S2 for a complete list of primers). The resulting cDNA was then digested with RNase cocktail (Invitrogen) at 37°C for 20 min and subsequently purified using AMPure XP beads (Beckman Coulter). A tailing reaction was then performed using dCTP and dATP (New England Biolabs). A second round of amplification was performed using gene-specific primers WhSBV-777-R (0.2 µM) and the AAP primer (0.2 µM) for purified C-tailed cDNA or the adapter primer (AP) (0.2 µM) for purified A-tailed cDNA (see Supplementary Table S2). The hemi-nested PCR was performed with gene-specific primers WhSBV-545-R (0.2 µm) and the AUAP primer (0.2 µm) (see Supplementary Table S2). To identify the 5' end, total RNA samples were treated with the *E. coli* Poly(A) Polymerase Kit (New England Biolabs) according to the manufacturer's instructions in order to add poly(A) tails. The poly(A) tailed RNA were then purified using AMPure XP beads. This purified poly(A) tailed RNA was used as input to the 3'-RACE system for rapid amplification of cDNA ends (Invitrogen), using the AP primer (see Supplementary Table S2) for RT-PCR. The cDNA was then digested with an RNase cocktail and purified using AMPure XP beads. For the second round of amplification, six different gene-specific primers (WhSBV_7388F, WhSBV_7528F, WhSBV_7911F, WhSBV_8215F, WhSBV_8737F, WhSBV_8901F; 0.2 µm) were combined with the AUAP primer (see Supplementary Table S2). The resulting PCR amplicons were separated by 2% agarose gel electrophoresis. The remaining product was purified with AMPure XP beads and sequenced using the BigDye Terminator v1.1 Cycle Sequencing Kit on a 3500 Genetic Analyzer (Applied Biosystems). The final WhSBV genome sequences were uploaded to Genbank under accession number PV171101.

RT-qPCR and qPCR assays for specific detection of WhSBV

For the following assays, persistently WhSBV-infected GSB and CiSB cells and the WhSBV-uninfected GK (0119) cell line (see Supplementary Table S1) were grown to 95-100% confluence in non-vented T25 tissue culture flasks using appropriate growth medium supplemented with 10% FBS. Cell pellets were harvested using Alsever's trypsin-versus-versus-solution (ATV; FLI, Riems) after discarding the supernatant, and RNA/DNA was extracted using the NucleoMag VET kit (Macherey-Nagel) according to the manufacturer's instructions.

WhSBV-specific reverse transcription quantitative polymerase chain reaction (RT-qPCR) assays were established by designing primers and probe sets targeting the viral N, P, G, M and L genes (see Supplementary Table S2, for a complete list of primers and probes). WhSBV-specific RNA (and potentially DNA) was detected using the AgPath-ID one-step RT-PCR reagents (Thermo Fisher Scientific). Briefly, 5 µl of extracted RNA was reverse transcribed and amplified in a reaction mix of 25 µl total volume containing the specific primer/probe mix (final primer and probe concertation: 0.4 and 0.2 µM, respectively). For the internal control, primers ACT-1030-F (final concentration: 0.2 µM) and ACT-1135-R (0.2 µM) along with probe ACT-1081-HEX (0.2 µM) were included in each reaction to target the cellular actin beta (*ACTB*) gene. The reaction was performed on a Bio-Rad CFX96 qPCR cycler (Bio-Rad) using the following cycling conditions: 45°C for 10 min, 95°C for 10 min, 42 cycles of 95°C for 15 s, 57°C for 20 s and 72°C for 30 s.

To exclude the presence of WhSBV sequences as endogenous viral elements (EVE) integrated into the cellular genome of GSB, CiSB, and GK, we specifically tested DNA extracted from these cells using a non-reverse transcription qPCR system. WhSBV cDNA from the 3'-RACE experiment, as previously described, was used as a positive control. The Maxima Probe/ROX qPCR Master Mix (Thermo Fisher Scientific) was used according to the manufacturer's protocol, targeting the viral genes N, P, G, M and L (final primer and probe concertation: 0.4 and 0.2 µM, respectively) and the cellular *ACTB* gene (final primer and probe concertation: 0.2 and 0.2 µM, respectively). The reaction was performed on a Bio-Rad CFX96 qPCR cycler using the following cycling conditions: 50°C for 2 min, 95°C for 10 min, 40 cycles of 95°C for 15 s, 60°C for 30 s and 72°C for 30 s.

Experimental infection of different cell cultures with WhSBV

Bony fish cells RT/F (CCLV no. 0088), CaPi (0112), EPC (0173), RTG-2/f (0686), CCB (0816), SAF-1 (0826), CHSE-214 (1104), GTS-9 (1388), ZF4 (1492), and TiB (1550), the

reptilian cells SKL-R (0484), VH-2 (1092), and CDSK (1536), the avian cells QM7 (0466) and DF-1 (1529), and the mammalian cells Vero (0015) and C6 (1452) were obtained from CCLV (see Supplementary Table S3 for a complete list of cell lines). All fish and reptile cell lines were grown in non-vented T25 flasks (Corning) to 95-100% confluence in an appropriate 10 ml growth medium supplemented with 10% FBS. Incubation temperatures were set at 20°C for the fish cells CHSE-214 and RTG-2/f, 26°C for all other fish cells and reptilian cell SKL-R, and 28°C for the reptile cells VH-2 and CDSK. Mammalian and avian cells were grown in vented T25 flasks at 37°C in a humidified atmosphere containing 5% CO_2.

For inoculum preparation, several non-vented T75 (75 cm²) culture flasks (Corning) containing persistently WhSBV-infected GSB cells with 5 ml of supernatant (equivalent to 1 ml of inoculum per 15 m² of infected cell layer) were frozen at -80°C and thawed three times. All supernatants were then combined into a single solution. To initiate the infection experiment, cells were grown to confluence in T25 flasks (25 cm²) as described above. Prior to inoculation (T0), 1 ml of supernatant was collected from each cell line. An equal volume (1 ml) of WhSBV inoculum was then added to the cultures (corresponding to an infection ratio of 1:1.7 between the area of the cell layer from which the inoculum originated and the area of the cell layer inoculated). Cultures were then incubated for one hour under the above conditions. After this incubation, a further 1 ml of supernatant was collected (T1). Cells were then incubated and split at regular intervals of 2-3 days at a 2-fold splitting factor for a total of 4-6 passages (P1-6). The splitting process involved collecting the supernatant before each passage, washing and detachment of the cells with ATV, and collecting half of the detached cells for analysis. The remaining cells were used for further culture by adding fresh growth medium supplemented with 10% FBS. The collected supernatants and cell pellets were stored at -80°C for subsequent RNA extraction and RT-qPCR analysis. Negative controls were treated in the same way as infected samples, except that the WhSBV inoculum was replaced by 1 ml RNase-free water (Qiagen). The infection experiment was performed in two independent runs for each cell line. As the infection of reptile, avian and mammalian cell lines was performed separately from the comparison of different fish cell lines, the cypriniform cell line GTS-9 was used as a positive control to validate the infectivity of the inoculum.

Nucleic acid extraction from supernatant and cell pellet samples was performed using the NucleoMag VET kit according to the manufacturer's instructions. The extracted nucleic acids were used for RT-qPCR analysis as described above, using the G gene-specific RT-qPCR primer/probe mix to monitor viral load and the ACTB primer/probe mix as an internal control for normalisation and to verify RNA integrity.

Electron microscopy

WhSBV-infected and uninfected ZF4 cells (see Supplementary Table S3) from the previous infection experiment were transferred to non-vented T75 flasks for electron microscopy analysis, along with the persistently WhSBV-infected GSB cells grown in non-vented T75 flasks. Cells were fixed in 2.5% glutaraldehyde buffered in 0.1 M sodium cacodylate pH 7.2 (SERVA Electrophoresis). 1% aqueous OsO_4 was used for post-fixation and 2.5% uranyl acetate in ethanol for *en bloc* staining (SERVA Electrophoresis). After a graded dehydration in ethanol, the samples were cleared in propylene oxide and infiltrated with Glycid Ether 100 (SERVA Electrophoresis). For polymerisation, samples were incubated at 60°C for 3 days. Ultrathin sections were transferred to formvar-coated nickel grids (slot grids; Plano). All grids were counterstained with uranyl acetate and lead citrate before examination on a Talos F200i transmission electron microscope (FEI) at an accelerating voltage of 80 kV.

Specific detection of viral RNA using RNA *in situ* hybridization

The cypriniform cell lines EPC and CCB and the non-cypriniform fish cells RTG-2/f and TiB (see Supplementary Table S3) were maintained in non-vented T75 flasks in a suitable medium supplemented with 10% FBS until they reached 95-100% confluence. Cultures were maintained under the conditions described in the previous infection experiment. For infection, 3 ml of medium was replaced with an equal volume of inoculum to achieve an infection ratio of 1:1.7, as previously described. Cells were harvested from two independent experiments at early and late time points: 0, 4, 8, 24, 48 hours post infection (hpi) for the early time points and 0, 72, 96, 120 and 240 hpi for the late time points. Harvesting was performed with a cell scraper (Sarstedt). The harvested cells were collected in 50 ml Falcon tubes (Sarstedt), centrifuged at 3500 rpm for 15 minutes and the supernatants discarded. The cell pellets were then fixed in 10% neutral buffered formalin (Carl Roth) for at least 24 hours. After paraffin embedding, 4-µm thick sections were processed for subsequent RNA *in situ* hybridisation (RNA ISH) using RNAScope 2-5 HD Reagent Kit Red and custom-designed probes targeting WhSBV (-)RNA (genomic RNA; WhSBV-L-O2, catalogue number 1567161-C1, Advanced Cell Diagnostics, Hayward, USA) on all samples according to the manufacturer's instructions. In addition, custom-designed probes targeting WhSBV (+)RNA (mRNA and antigenomic RNA; WhSBV-G-O1, catalogue number 1567171-C1) were used on CCB samples. As technical controls, probes against the genes for peptidylprolyl isomerase B (PPIB) and dihydrodipicolinate reductase (DapB) were included in each run. All pages were scanned using a Hamamatsu S60 scanner and evaluated using NDPview.2 plus software (version 2.8.24, Hamamatsu Photonics, K.K. Japan) by a board-certified pathologist (AB, DiplECVP). The abundance of infected cells was recorded as a percentage in a 10 × 10 grid (size 100 ×

100 µm per grid cell). Thus, a positive signal within a grid cell resulted in one percentage point. The distribution pattern of the viral RNA was also scored using a “pattern score”: 0 = none; 1 = chromogenic labelling in single cells; 2 = labelling in cell clusters; 3 = labelling in confluent cell clusters; 4 = diffuse labelling. Finally, the size of the chromogenic signal was determined as “signal score”, 1 = fine-granular or 2 = globular. The total pattern/signal score was calculated as the sum of the signal and pattern scores.

In a separate kinetics experiment to correlate with the RNA ISH results, the same cell lines as above were seeded in 12-well plates (3.8 cm^2 cell layer per well) (Corning) and maintained to 95-100% confluence in appropriate medium supplemented with 10% FBS. Cultures were maintained at 26 or 20°C (for RTG-2/f) and 5% CO_2. Inoculation was performed at a 1:0.8 infection ratio as described above, with 300 µl of medium replaced by 300 µl of WhSBV inoculum. Infection of each cell line was performed in three independent replicate wells for each time point. Cell pellets were harvested at 0, 4, 8, 24, 48, 72, 96, 120, 144, 168, 192, 216 and 240 hpi. At each time point, supernatants were discarded and cell pellets were collected by trypsinisation using ATV. RNA was extracted using the NucleoMag VET kit as described previously. RT-qPCR was then performed using G gene and ACTB specific RT-qPCR primer/probe mixes.

Gene expression analysis of early and late WhSBV infection

The CCB cells (see Supplementary Table S3) were used to study the effect of WhSBV on cellular gene expression. Cells were seeded in 6-well plates (9.6 cm^2 cell layer per well) (Corning) and cultured for 24 hours to 95-100% confluence in 10% FBS supplemented medium. They were maintained under the conditions described in the previous kinetics experiment. Infection with WhSBV was performed at a 1:1.3 ratio as described above by replacing 500 µl of culture medium in each well with 500 µl of WhSBV inoculum. Negative controls were inoculated with 500 µl of the same medium used for persistently WhSBV-infected GSB cultivation, replacing 500 µl of the cell culture medium. Cell pellets were collected in two independent experiments to assess early and late infection stages. In the early infection experiment, mock-infected and WhSBV-infected cell pellets were collected at 4, 8, 24 and 48 hpi. For the late-stage experiment, samples were collected at 72, 96, 120 and 240 hpi. In addition, pre-infection cell pellets were collected at 7 and 24 before inoculation, the latter representing the 0 hpi time point. Infection was performed in three independent replicate wells for each time point. Cell pellets were collected by trypsinisation after supernatants were discarded. Total RNA was extracted using Trizol, chloroform and the Agencourt RNAdvance Tissue Kit as previously described. RT-qPCR was performed on all samples using G-gene and ACTB-specific RT-qPCR primer/probe mixes to validate samples

prior to sequencing. Transcriptomic libraries were prepared as previously described, but including ERCC spike-in mix (Invitrogen) as an internal control. Subsequently, the libraries were pooled and sent for sequencing on an Illumina NovaSeq 6000 system (Novogene GmbH) running in paired-end 150 bp mode. Raw reads were subsequently trimmed using *TrimGalore!* (v0.6.10) and then analysed using the nf-core RNAseq pipeline (version 3.14.0; (Ewels et al. 2020)). In detail, the common carp reference genome GCF_018340385.1 was used for splice-aware mapping with STAR and subsequent quantification with salmon. The quantification data was then further analysed in R (v4.3.1) and differentially expressed genes (DEGs) were deduced using the DESeq2 package (v1.40). Log2-fold changes were shrinked using the function “lfcShrink”. The cut-off values for DEGs were set to absolute shrinked log2-fold change > 1 and adjusted *p-value* < 0.05. To explore global gene expression patterns, principal component analysis (PCA) was performed using R. Transcriptomic data have been deposited in ArrayExpress under E-MTAB-14894.

Validation of predicted splice sites in WhSBV genome

The trimmed raw reads from the metagenomic RNA datasets from persistently WhSBV-infected GSB and CiSB cells (see Supplementary Table S1) were mapped back to the respective WhSBV genomes using the generic mapper Geneious Prime with medium sensitivity settings (options: find structural variants, short insertions and deletions of any size) to visualise the transcriptional profile of WhSBV and predict potential splice sites and introns. To experimentally validate each predicted splice site, primers were designed to amplify the specific genomic regions by RT-PCR. MEME (v5.5.2) was used to predict the conserved motifs of potential transcription start and termination sites.

Purified RNA was extracted by RNeasy Mini kit as described above. cDNA from poly(A) RNA was synthesized using the Protoscript II First Strand cDNA Synthesis Kit and oligo-dT primers (New England Biolabs). The cDNA products were then digested with an RNase cocktail and purified using AMPure XP beads. Conventional Taq-PCR was performed using the Accuprime *Taq* DNA Polymerase System (Invitrogen) with primers specific for the predicted splice sites within the viral M and L genes (see Supplementary Table S2). RNase-free water was used instead of cDNA as a negative control. The amplified DNA products were run on a 2% agarose gel and bands were excised. The DNA was extracted using a QIAquick Gel Extraction Kit (Qiagen) and then sequenced using the BigDye Terminator v1.1 on a 3500 Genetic Analyzer.

Specific detection of viral RNA using Northern blot

RNA was extracted from the persistently WhSBV-infected GSB, WhSBV-infected and uninfected EPC cells (see Supplementary Tables S1 and S3) from the previous infection experiment using the TRIzol-chloroform method and the RNeasy Mini Kit with DNase I as previously described. RNA quality and quantity were assessed using the Agilent Tapestation 4150 and NanoDrop Lite spectrophotometer as described previously. Subsequently, 2-4 µg of total RNA was glyoxylated (Glyoxal, Sigma-Aldrich) at 56°C for 45 min before separation on a 0.9% denaturing agarose gel (4.7% formaldehyde, Carl Roth) in a phosphate buffer system. RNA was transferred overnight to Hybond-N membranes (Cytiva Amersham) using SSC transfer buffer. RNA was cross-linked to the membrane and viral RNA (mRNA and genomic RNA) was detected using DNA probes. Probes were generated by RT-PCR using specific forward and reverse primers against each gene of WhSBV (see Supplementary Table S2) using the Platinum Script III One-step RT-PCR Kit (Thermo Fisher Scientific) according to the manufacturer's instructions. The amplified cDNA products were then run on a 2% agarose gel. After amplification, the products were purified using AMPure XP beads according to the manufacturer's protocol. The quantity of purified products was measured using a NanoDrop Lite spectrophotometer and labelled with ^{32}P-CTP (Hartmann-analytic) using a Nick translation kit (GE Healthcare). Hybridisation was performed overnight at 60-65°C and the signal was analysed after washing using the CR35 phosphoimager system (Dürr medical).

Specific detection of WhSBV proteins

Approximately 3×10^5 persistently WhSBV-infected GSB cells were harvested, resuspended in 1× LDS Buffer (Thermo Fisher Scientific) containing 100 mM DTT (Sigma-Aldrich) and heated for 10 min at 70°C shaking at 1400 rpm in a Thermomixer (Eppendorf). Reconstitution buffer (50 mM HEPES/KOH, pH 7.5, 100 mM NaCl, 1 mM EDTA, pH 8.0, 0.5% [w/v] Sodium deoxycholate, 1% [v/v] Triton X-100) was added to a final volume of 100 µl. Samples were reduced in 10 mM DTT for 30 min at 60°C followed by alkylation in 25 mM iodoacetamide (Sigma-Aldrich) for 25 min at RT in the dark with orbital shaking at 800 rpm in a Thermomixer (Eppendorf). The reaction was quenched by incubation with 10 mM DTT f.c. for 5 min at RT. For protein binding 125 µg hydrophilic and 125 µg hydrophobic Sera-Mag Carboxylate-Modified Magnetic Particles (GE Healthcare) together with 150 µl absolute ethanol (Carl Roth) were added to each sample and incubated for 15 min at RT at 1000 rpm in a Thermomixer (Eppendorf). Beads were washed three times with 80% LC/MS grade ethanol (Supelco, Inc.). Residual ethanol was removed prior to adding 1 µg LC-grade trypsin (Serva) in 100 µl of 50 mM ammonium bicarbonate buffer pH 8. After incubation for 4 h at

37°C and 1000 rpm in a Thermomixer (Eppendorf) peptides were collected and desalted on StageTips (Rappsilber et al. 2007). The amount of 400 ng digested peptides were analyzed with a nanoElute2 HPLC system (Bruker) coupled to a TimsTOF HT mass spectrometer (Bruker). Peptides were separated on an Ultimate CSI 25×75 C18 UHPLC column (Ionopticks) by running an optimized 100 min gradient of 2 to 95% MS-grade acetonitrile with 0.1% formic acid at 250 nl/min at 50°C. The mass spectrometer was operated with the manufacturer provided DDA_PASEF_1.1sec_cycletime method. Mass spectrometry raw files were processed with MaxQuant (version 2.4.13.0) (Cox and Mann 2008) using a custom virus database (6 entries) and the *C. idella* database (C_idella_female_genemodels.v1; 32,811 entries) with standard settings.

RESULTS

Metagenomic screening of different fish cell lines reveals presence of WhSBV

During metagenomic sequencing of 48 fish cell lines, the cypriniform cell lines GSB and CiSB were found to contain WhSBV sequences (Supplementary Figure S1). Complete viral genomes were assembled from both cell lines, sharing 99.9% nt identity with each other and 99.9% and 87.8% nt identity with WhSBV variants CIK (BK063520) and DSYS4497 (NC_055169), respectively. The initial assembly identified a WhSBV genome sequence of 8,985 nt in length. However, 3' and 5' RACE extended the initial genome to 9,008 nt (Supplementary Figure S2). Compared to the current WhSBV reference sequence in Genbank (RefSeq NC_055169), the complete WhSBV genome sequence presented here is 13 and 10 nt longer at the 3' and 5' ends, respectively.

Using the complete WhSBV genome sequences, gene-specific RT-qPCR assays targeting the N, P, G, M, and L gene regions were established. Among these, the G gene-specific RT-qPCR assay was selected for screening all the 48 fish cell lines, as it showed best sensitivity. The assay yielded positive results for GSB and CiSB cell lines with Cq values of 18.9 and 19.4, respectively, while all other tested cell lines tested negative for the WhSBV G gene (see Supplementary Table S1). In GSB and CiSB, N, P, M, and L gene assays were also positive by RT-qPCR (see Supplementary Figure S3), while no signals were detected in the negative control cell line GK. Furthermore, qPCR assays targeting the WhSBV N, P, G, M and L gene regions without prior reverse transcription were negative for GSB and CiSB cells, indicating that the detected WhSBV sequences are unlikely to originate from EVEs integrated into the host genome, but rather represent viral RNA (see Supplementary Figure S3).

WhSBV replicates in fish and reptilian but not in avian and mammalian cells

In order to test the infectivity of the identified WhSBV and its potential *in vitro* host range, we used cell lysate from persistently WhSBV-infected GSB cells to inoculate various cell lines from bony fish, reptiles, birds and mammals (see Supplementary Table S3). Following inoculation, the cells were propagated for several passages, and both cell pellets and supernatants were tested for presence of viral RNA using the established G gene-specific RT-qPCR assay. An RT-qPCR assay targeting the cellular ACTB gene was used as a baseline and extraction control.

WhSBV RNA was detected in the supernatant and cell pellet of all fish cell lines tested during the first one to two passages. In cells from the order Cypriniformes, including cyprinid (CaPi,

CCB and GTS-9), leuciscid (EPC) and danionid (ZF4) species, viral RNA was retained over all six consecutive passages. The amount of viral RNA detected started to increase compared to freshly inoculated cells (T1) and eventually reached a plateau at around Cq 25 in both supernatant and cell pellet. This stabilisation occurred between passages 2 and 4 for the CaPi, EPC, CCB and GTS-9 cell lines. For zebrafish cell line ZF4, the amount of viral RNA initially decreased after inoculation and passaging until passage 2-3, but then recovered, reaching Cq values of about 28 in supernatant and cell pellets (**Figure 1A**).

In contrast, the non-cypriniform fish, centrarchid (RT/F), and sparid (SAF-1) showed no evidence of WhSBV replication after inoculation (**Figure 1B**). Immediately after inoculation (T1), viral RNA levels in the supernatant were similar to those of the cypriniform cell lines (**Figure 1A**), but dropped below the detection limit in cell pellets and supernatant at passage 2-3 (**Figure 1B**). The chichlid (TiB) and salmonid (RTG-2/f and CHSE-214) cell lines showed a decrease in cell growth, which was also reflected in the measured ACTB RNA levels, leading to a complete loss of the salmonid cultures after passage 4. Viral RNA was still detectable in the cell pellets until the loss of the cultures or the end of the experiment, but without a detectable increase in levels (**Figure 1B**).

In the reptilian cell lines SKL-R, VH-2, and CDSK, viral RNA levels in the supernatant decreased after inoculation but stabilised at around Cq 32-38 and remained detectable up to passage 6 (**Figure 2**). In the SKL-R cell pellet, WhSBV RNA was detectable at similarly low levels up to passage 6. In the CDSK and VH-2 cells, viral RNA levels increased during passages 5 and 6, reaching Cq values of 29 and 30, respectively.

In the mammalian Vero and C6 cell lines and the avian QM7 and DF-1 cell lines, WhSBV RNA levels in the cell pellets or supernatants dropped below or near the detection limit already after passage 1 or 2, respectively (**Figure 2**).

All negative controls used in this experiment showed no Cq values for the viral glycoprotein.

No apparent cytopathic effect was observed in any of the cell cultures used throughout the experiment.

Using transmission electron microscopy, we detected virion-like structures in WhSBV-inoculated ZF4 cell lines, whereas similar structures were absent in non-inoculated controls. The putative WhSBV virions are spherical to pleomorphic with a diameter of approximately 150-180 nm (**Figure 3A**). Virion budding was observed rarely at the plasma membrane of the persistently WhSBV-infected GSB cells (**Figure 3B**).

Progressive increase of viral RNA in cypriniform cell lines over time

In order to gain deeper insights into viral propagation in different fish cell lines, a kinetic experiment was performed over 10 days using both cypriniform (EPC and CCB) and non-cypriniform fish cells (RTG-2/f and TiB). The level of viral RNA load was assessed by RT-qPCR and the presence of viral RNA at the cellular level was assessed by RNA ISH at different time points.

In the cypriniform EPC and CCB cell lines, the virus exhibited almost identical exponential growth curves, with viral RNA levels increasing from 12 hpi and reaching Cq values of 18.6 for EPC and 19.5 for CCB. In contrast, the salmonid RTG-2/f and cichlid TiB cell lines showed stagnation or a gradual decrease in detectable viral RNA levels (**Figure 4A**).

The presence of viral RNA in the cells was detected by specific RNA ISH, which detects viral (-)RNA in both cypriniform (EPC and CCB) and non-cypriniform fish cell lines (RTG-2/f and TiB) from 4 hpi. In general, RNA ISH confirmed the results of the kinetic experiment based on the RT-qPCR assay. In particular, initial visual inspection of the cypriniform cell lines revealed that the number of infected cells was higher at later time points. At early time points (4 - 72 hpi), infected single cells appeared, followed by foci of positive cells, later confluent and finally diffuse labelling of the cell pellet (**Figure 4B**). Percentage quantification of individual cell pellets for EPC showed widespread infection, with 95% of the fields analysed showing positive detection as early as 4 hpi. Infection remained widespread (63-100% of infected test fields) throughout the course of the experiment until 240 hpi (see Supplementary Figure S4). In CCB cells, only 29% of the test fields were infected at 4 hpi and longer cultivation correlated with a higher proportion of positive test fields, eventually reaching 100% at 96, 120 and 240 hpi (see Supplementary Figure S4). Similar observations were made using a custom-designed probe against WhSBV (+)RNA on CCB cell lines (Supplementary Figure S5). In terms of labelling signal, infected cells harvested at early time points were more likely to show fine-granular cytoplasmic labelling, and larger, globular signals were consistently found at 48 hpi and later (**Figure 4B**). In clear contrast, the infection pattern in the non-cypriniform fish cell lines were essentially confined to single cells and showed no evidence of increasing infection abundance over time (**Figure 4B**). Only the intensity of the chromogen signal within the cell increased in TiB from 72 hpi, but in RTG-2/f this phenomenon was limited to 72 and 96 hpi. RTG-2/f and TiB cells ultimately yielded 28% and 16% infected test fields at 240 hpi, respectively (see Supplementary Figure S4).

Cellular response to early and late WhSBV infection is limited in cypriniform cells

To investigate cellular transcriptional changes associated with WhSBV infection, we performed RNA sequencing (RNAseq) of RNA transcripts at early and late time points following viral inoculation in CCB cells (**Figure 5A**). Quantitative RT-qPCR and sequencing confirmed the presence of WhSBV RNA and the onset of infection at 4 hpi, with viral RNA levels progressively increasing at all subsequent time points (**Figure 5B**). This trend was consistent with the RNA ISH data, which showed a gradual increase in the percentage of infected CCB cells over time, reaching 100% infection at 96, 120, and 240 hpi (**Figure 5B**).

The number of DEGs remained minimal at early and late time points but became more pronounced at 240 hpi, indicating a delayed transcriptional response to infection (**Figure 5C**). PCA of early time points revealed clear transcriptional differences between WhSBV-infected and control cells at 4 and 8 hpi, which diminished at 24 and 48 hpi, with both groups becoming more similar (**Figure 5C**). In contrast, the PCA of late time points experiment showed no significant transcriptional changes at 72 and 96 hpi, However, minimal transcriptional alterations were observed at 120 hpi, followed by distinct clustering of infected and control samples at 240 hpi, suggesting a change in the host transcriptional response at later stages of infection (**Figure 5D**).

Differential gene expression analysis of early time points identified three DEGs at 4 or 8 hpi. Specifically, RASAL2 (RAS GTPase-activating protein 2-like [LOC109087896]) and IRF1B (interferon regulatory factor 1) were upregulated at 4 hpi and 8 hpi (**Figure 5E**), whereas EDEM3 (ER degradation enhancing alpha-mannosidase-like protein 3 [LOC109095466]) was upregulated exclusively at 8 hpi. Conversely, ABCC1 (multidrug resistance-associated protein 1-like [LOC109090229]) was downregulated at 4 hpi. The expression of these genes returned to baseline levels by 24 and 48 hpi. At later stages of infection (72 and 96 hpi), no DEGs were detected between infected and control cells. At 120 hpi, eight DEGs were upregulated, including IRF7 (interferon regulatory factor 7) and MxB (interferon-induced GTP-binding protein MxB-like) (**Figure 5E**). At 240 hpi, 113 DEGs were upregulated, including IRF7, MxB, and several other key antiviral genes involved in early innate immune responses in fish, such as IRF3 (interferon regulatory factor 3), ISG15 (interferon-stimulated gene 15), and RSDA2 (viperin, radical S-adenosyl methionine domain containing 2), along with other genes involved in interferon pathways, RIG-I (antiviral innate immune response receptor RIG-I [LOC109081892]) and GVINP1 (interferon-induced very large GTPase 1-like [LOC109058642]) (**Figure 5E** and Supplementary Table S4 for complete list of DEGs).

Detection of multicistronic and spliced WhSBV gene transcripts

To investigate the transcriptional profile and splice sites of the WhSBV RNA, we mapped raw sequence data from the persistently WhSBV-infected GSB and CiSB cells to the de novo assembled WhSBV genome (**Figure 6A**). The observed sequence coverage across the genomes was uneven, with abrupt increases and decreases observed in certain potential intergenic regions. These coverage variations corresponded to predicted transcription start and stop motifs. Three transcriptional start sites (S1-3) were identified upstream of the N, X/P and M ORFs. Start sites were marked by a significant increase in read coverage, indicating transcription initiation. Four transcription termination sites (T1-T4) were detected, T1, T2 and T4 were located downstream of the N, G and L ORFs, respectively, while T3 was found within the L ORF. The termination sites were characterised by a decrease in read coverage and the presence of reads transitioning to poly(A) tails, consistent with transcriptional termination (**Figure 6A**). S2 and S3 are observed immediately adjacent to T1 and T2, respectively. The predicted start and termination motifs showed a conserved sequence pattern (see Supplementary Table S5). As the 5' RACE analysis was performed on total RNA including mRNA, Sanger sequencing of some 5' RACE products identified the transcription start site S1 at nucleotide position 33 to 35 in the viral genome, marked by the sequence “GAA”, in agreement with the prediction results.

Regions of the genome with comparable levels of sequence coverage between adjacent start and termination sites were interpreted as belonging to the same viral RNA transcript or mRNA. Briefly, the N gene appeared to be expressed from a monocistronic mRNA, while X/P and G genes were expressed from polycistronic mRNA. The mRNAs containing the M and L genes shared a common start site (S3); however, their transcript levels differed with the M gene being more highly expressed than the L gene (**Figure 6A**).

In addition, mapping revealed the presence of three potential introns (In1-3) located at the beginning of the L ORF. Conventional RT-PCR and Sanger sequencing confirmed the presence of In1-3 within the L ORF and also revealed an additional, unpredicted splice site, In4, within the L ORF (**Figure 6B**).

Based on the above findings, we predicted several potential transcripts for the M and L genes, which share the same start site S3 and terminate at either T3 or T4. The M gene could produce a short transcript encoding the M ORF, which can either remain unspliced (M t1; size: 741 nt) or undergo splicing at In1 to produce a shorter transcript (M t2; 565 nt), both terminating at T3. However, the unspliced transcript appears to be in the minority of transcripts or non-existent, as mapping suggests truncation at the In1 region. In addition, four transcripts were predicted, termed M-L t1-4, all sharing the same start site S3 and

termination site T4, but differing in their splicing patterns. The longest unspliced transcript, M-L t1, contains the full-length M and L ORFs (5,680 nt), whereas the other transcripts (M-L t2-4) are progressively truncated by splicing at different introns, resulting in transcripts of size 5,218 nt, 5,150 nt, and 4,945 nt, respectively (**Figure 6C**). These transcripts may encode either truncated versions of the L ORF or only the M ORF.

A complementary northern blot analysis of RNA from the persistently WhSBV-infected GSB and the uninfected and experimentally WhSBV-infected EPC cells, supported these findings (**Figure 7A-C**). All probes (N, X, P, G, M, or L ORF specific) detected the full genome of WhSBV from the GSB and EPC cells at the expected size of 9,008 nt. X, P and G are encoded by the same RNA, as all three probes detected the same RNA species at approximately the predicted size of 2,118 nt. This is consistent with their expression from polycistronic mRNA. The M and L probes both detected a band between 6 and 8 kb, likely representing the M-L t1 transcript. A faint band at 500 nt was detected with the M probe, but not with the L probe, which may represent the short transcripts of the M ORF. The N probe identified an RNA species that was consistently higher than expected and was also recognised by the X, P and G probes. This observation suggests the presence of a long RNA spanning all four ORFs, rather than the expected monocistronic N ORF mRNA.

High-resolution mass spectrometry was performed on the GSB cell suspension persistently infected with WhSBV to provide an overview of the viral proteins. The analysis revealed peptides that matched all the predicted proteins of WhSBV, except for the L ORF where no matching peptides were detected. No fused peptides were detected either, suggesting no additional splicing (**Figure 8**).

DISCUSSION

This study represents the first *in vitro* molecular characterisation of Wǔhàn sharpbelly bornavirus (WhSBV), a member of the family *Bornaviridae*, genus *Cultervirus* (Rubbenstroth et al. 2021; Shi et al. 2018), and thus the first biological characterisation of a bornavirus not belonging to the well-studied genus *Orthobornavirus*. Initially, identified by RNA sequencing of sharpbelly tissues (gut, liver and gill) (Eshak et al. 2023; Shi et al. 2018), WhSBV was later detected by data mining in grass carp cell lines (CIK and L8824) (Eshak et al. 2023; Shi et al. 2018; Costa et al. 2021). Here, we further identified WhSBV in two grass carp swim bladder-derived cell lines by metagenomic RNA sequencing. Both cell lines were originally established by the Pearl River Fisheries Research Institute (PRFRI), Guangzhou, China. Despite their extensive use in grass carp reovirus research (Liang et al. 2014; Yang et al. 2021; Ma et al. 2011), these cell lines had not previously been associated with WhSBV. Whether the cells used to establish the cell lines were harvested from an WhSBV-infected animal or were contaminated during handling from an unknown source remains unknown. While contamination can't be completely ruled out, the fact that WhSBV replicates and persistently infects cypriniform cell lines suggests that the virus is more likely to have originated from the grass carp used for the cell culture. This suggests that WhSBV may be endemic in cypriniform fish, such as grass carp and sharpbelly fish.

The identification of WhSBV in well-established cell lines allowed us to study the virus *in vitro*, offering insights into WhSBV persistence, potential *in vitro* host range, and transcriptional strategies. By comparing its ability to replicate in cypriniform cell lines, we demonstrated that WhSBV establishes a persistent infection without inducing cytopathic effects and maintains stable viral RNA levels over multiple passages (**Figure 1A**). Similar behaviour has been observed for BoDV-1, BoDV-2, VSBV-1 and several avian orthobornaviruses, where some inoculated cell lines became persistently infected without cytopathic effect and could be sub-cultivated without loss of infectivity (Herzog and Rott 1980; Rinder et al. 2009; Pham et al. 2020; Rubbenstroth et al. 2012; Rubbenstroth et al. 2014; Rubbenstroth et al. 2013; Schlottau et al. 2020; Nowotny et al. 2000). The efficient replication in cypriniform cells and the ability to establish persistent infections may indicate that fish of this order are the preferred host of WhSBV in natural environments. However, the natural host range of WhSBV and other culterviruses remains unknown.

To assess the infectivity of WhSBV in different cell lines, we inoculated cell lines from different taxonomic groups, including non-cypriniform fish, reptiles, birds and mammals. In

some non-cypriniform fish cell lines, susceptibility to WhSBV infection was difficult to assess because a decline in ACTB levels over several passages, with eventual loss of cultures, suggested suboptimal growth conditions, possibly due to excessive passaging or the use of non-vented flasks. In others, however, viral RNA was lost after a few passages despite stable ACTB levels, suggesting that they did not facilitate persistent WhSBV infection (**Figure 1B**). Despite these limitations, RNA ISH confirmed the presence of viral RNA within cells for RTG-2/f and TiB, indicating that these cells were indeed infected by WhSBV. However, infection remained confined to individual cells and there was no progressive increase in the percentage of infected cells, unlike in cypriniform cells where infection spread over time. Surprisingly, WhSBV was able to infect, replicate and establish persistence in all reptilian cell lines tested, albeit with lower viral RNA levels compared to the positive control, cypriniform GTS-9 fish cells (**Figure 2**). However, similar declines in ACTB levels were observed as in non-cypriniform fish. No sustained replication of WhSBV was detected in either avian or mammalian cell lines, as viral RNA levels declined rapidly and were undetectable after several passages (**Figure 2**). This may be due either to the absence of essential host factors in avian or mammalian cells required for WhSBV replication, or to an effective antiviral response.

The limited ability of WhSBV to infect and replicate in non-cypriniform fish and reptilian cells may indicate an evolutionary history of adaptation to these hosts, and therefore the potential existence of other related culterviruses with a greater affinity for these hosts. An *in silico* screening identified five novel fish bornavirids in bony and cartilaginous fish hosts that showed significant genomic divergence, suggesting that the diversity of culterviruses is currently underestimated (Eshak et al. 2023). Future studies will be essential to determine host range of WhSBV and other *Cultervirus* members in natural settings.

In order to study how WhSBV is able to establish a persistent infection without inducing cytopathic effects, we analysed the host gene expression at different time points of infection. Transcriptomic analysis of the experimentally WhSBV-infected CCB cells indicated a limited initial activation of the innate immune response shortly after inoculation at 4 and 8 hpi by upregulation of the genes IRF1B and RASAL2 (**Figure 5E**). Interferon regulatory factors, such as IRF1B, are key regulators of the innate antiviral response in vertebrates, controlling the expression of interferons (IFNs) and interferon-stimulated genes (ISGs) (Nehyba et al. 2009; Negishi et al. 2018). In zebrafish, IRF1B alone was shown to induce the expression of interferon and ISGs, resulting in effective protection against viral infection (Feng et al. 2015). While the role of RASAL2 in fish is currently unknown, the gene may function as tumour and metastasis suppressor in humans (McLaughlin et al. 2013). Despite the initial expression of IRF1B, no significant host cell transcriptional changes were observed between 24 and 96 hpi

(**Figure 5C**), possibly allowing for efficient viral replication and spread (**Figure 5B**). The lack of significant host cell transcriptional changes between 24 and 96 hpi is in stark contrast to the observed rising levels of viral RNA and high percentage of infected cells.

In comparison, orthobornaviruses have been shown to evade IFN induction by possessing monophosphorylated genome ends (Habjan et al. 2008; Reuter et al. 2010). BoDV-1 further suppresses the interferon response via P-protein-mediated inhibition of TANK-binding kinase 1 (TBK-1) (Unterstab et al. 2005) and N-protein interference with IRF7 activation (Song et al. 2013).

Only at 72 hpi we observed the activation of IRFs other than IRF1B, that resulted in a delayed innate immune response at 120 and 240 hpi, characterised by the significant upregulation of many ISGs, such as MxB, GVINP1, ISG15, and RSDA2, which play a role in the innate antiviral response in fish (Del Ortega-Villaizan et al. 2022). This suggests that the host's innate immune system did not mount a response until the infection had spread to all cells. However, this response was ultimately ineffective, as the cells remained persistently infected, possibly indicating the presence of a secondary regulatory mechanism controlling viral load. Despite the upregulation of ISGs, no significant induction of apoptosis- or necrosis-related genes was observed throughout infection, suggesting that WhSBV establishes persistence without inducing programmed cell death. This allows for continued viral replication and long-term infection. In contrast, common carp hepatocytes exposed to ammonia stress undergo apoptosis via the P53-BAC/BCL-2 pathway, demonstrating the species' ability to induce cell death under certain conditions (Xue et al. 2021). The absence of such responses in WhSBV-infected cells raised the possibility that the virus actively suppresses apoptosis, further contributing to its persistence. In fish, there is ongoing debate regarding the classification of their IFNs as type I, II, or III due to the presence of introns in fish IFN genes. However, phylogenetic and structural analyses suggest that fish IFN genes primarily encode type I IFNs (Qi et al. 2010; Hamming et al. 2011; Chang et al. 2013). Type I IFNs are known to trigger a cascade of immune responses upon viral infection, leading to the induction of antiviral genes (Huang et al. 2015; Chang et al. 2013). Interestingly, despite the induction of ISGs, type I IFNs (e.g. IFNA3) were not among the upregulated DEGs (**Figure 5E**). This suggests the involvement of alternative signalling pathways in common carp or very subtle IFN expression. Additionally, certain viral pathogens have evolved mechanism to suppress host interferon signalling, which could explain the absence of type I IFN upregulation (Swaraj and Tripathi 2024). Further studies are needed to elucidate the molecular mechanisms underlying WhSBV-mediated immune evasion and/or modulation and to identify the specific viral genes, proteins or genomic structures involved in these processes. The establishment of persistence without cytopathic effects is a common feature

of orthobornaviruses (Rubbenstroth et al. 2021) and has also been observed in other mononegaviruses, such as arenavirids (family *Arenaviridae*), which suppress host antiviral responses, particularly by inhibiting type I interferon production, to maintain chronic infections (Meyer and Ly 2016; Kane et al. 2016).

In order to regulate its own gene expression, WhSBV shares conserved transcriptional features with other *Cultervirus* genomes, notably the presence of an intron at the boundary between the M and L genes, suggesting a common transcriptional mechanism. Additionally, culterviruses have a conserved nucleotide sequence pattern for termination sites (T1-T4), “AYUUWAKAAAAACAU“, while start sites (S1-3) follow the motif “GAM” (Eshak et al. 2023). However, experimental validation of these transcriptional elements is still required. In contrast to the predominantly monocistronic transcription seen in other mononegaviruses (Amarasinghe et al. 2019), such as paramyxovirids (family *Paramyxoviridae*), where the viral genome is transcribed into monocistronic mRNAs, each encoding a single protein (Wignall-Fleming et al. 2019). Orthobornaviruses use polycistronic mRNAs with extensive splicing of the overlapping M, G, and L ORFs to regulate their gene expression (Cubitt et al. 1994; Cubitt et al. 2001; Schneider et al. 1994; Tomonaga et al. 2000), along with multiple transcriptional start and termination sites, as observed in BoDV-1 (Tomonaga et al. 2002; Schneider et al. 1994). In WhSBV, the M and G ORFs have been repositioned during evolution and splicing events occur at the M-L boundary. Understanding the differences in splicing patterns may provide insight into the evolutionary forces shaping genome organisation and how each genus regulates transcription in different host species. There is currently no data is available on the splicing patterns of carboviruses, which share the same genome organisation as culterviruses. Determining whether they exhibit similar or distinct transcriptional mechanisms is essential to understanding their different regulatory strategies (Hyndman et al. 2018). Notably, bornavirids are not the only mononegaviruses that use polycistronic transcription; for example, Ebola virus (EBOV; family *Filoviridae*) uses RNA editing of its glycoprotein (GP) gene to generate multiple GP variants, optimising replication and pathogenicity without increasing genome size (Yu et al. 2017).

Northern blot analysis suggested that the N proteins can be expressed not only from a monocistronic mRNA, but also co-expressed with the X/P and G from a polycistronic mRNA. However, it remains to be clarified whether the detected RNA of approximately 3000-4000 nt in length is actually mRNA or a subgenomic RNA. For BoDV-1, the non-coding region between the N and X genes shows structural similarities to that of WhSBV, where T1 is located downstream of the transcription start site S2 (Poenisch et al. 2008). The consensus motif of the BoDV-1 termination sites, $U(A)_{6\text{-}7}$ (Schneemann et al. 1995), serves as a core signal sequence but is insufficient for efficient transcription termination on its own, as the

surrounding upstream and downstream nucleotides significantly influence T1 utilization. Consequently, when transcription is initiated at S1 and terminated at T1, these regulatory elements contribute to the production of a monocistronic (1,200 nt) mRNA encoding the N protein (Poenisch et al. 2008). However, studies have demonstrated that the viral transcriptase frequently bypasses the T1 transcription termination site, resulting in the production of a longer (1,900 nt) polycistronic mRNA containing the N, X, and P ORFs (Poenisch et al. 2008). The presence of such transcripts in BoDV-1-infected cell cultures and rat brains suggests that they are bona fide mRNAs rather than aberrant replication intermediates, and their production may be related to viral fitness (Poenisch et al. 2008). Conversely, other studies have suggested that these long mRNAs may represent aborted replication products or an extended form of “leader RNA”, similar to those described in certain other negative-strand RNA viruses (Schneemann et al. 1994; Banerjee et al. 1991). In addition, although L transcripts were detected by Northern blot, proteomic analysis did not identify L protein, suggesting low levels of expression, possibly regulated by splicing events that modulate its protein level, similar to BoDV-1 (Schneider et al. 1994). A similar mechanism has been observed for vesicular stomatitis virus (VSV; family *Rhabdoviridae*), which controls L gene expression by polycistronic transcription, co-expressing it with other viral genes to balance protein levels and minimise host cell stress while optimising viral replication and assembly (Barr et al. 2002). This specific transcriptional regulation of WhSBV may balance viral protein levels but requires further investigation.

CONCLUSION

This study provides a molecular characterisation of WhSBV, suggesting an adaptation to predominantly cypriniform hosts and its ability to establish a persistent infection without inducing detectable cytopathic effects. The efficient replication of the virus in cypriniform cell cultures and the suppressed induction of an early host innate immune response underline its evolutionary co-adaptation to these fish hosts. Our findings highlight the importance of moving from *in silico* screening to *in vitro* validation, a critical step in virological research. While metagenomic approaches facilitate virus discovery, the lack of direct sequence validation from real samples often remains a key limitation. Furthermore, the ability of WhSBV to establish persistent infections in cypriniform cells, while showing limited replication in non-cypriniform cultures, highlights the need for *in vivo* experimental validation in defining viral host ranges. In addition, this study provides valuable insights into the transcriptional mechanisms of WhSBV, highlighting its regulatory strategies to modulate gene expression. Further research is essential to unravel the molecular mechanisms underlying the persistence of WhSBV and to assess its ecological impact, particularly in

aquaculture where persistent viral infections could have significant implications for fish health and disease management.

DATA AVAILABILITY

All sequencing data associated with this study have been deposited in public repositories and are freely accessible. The genome sequence is available in GenBank under the accession number PV171101. Additional metadata can be found under BioProject PRJNA1226401 and BioSample SAMN46928747. Raw sequencing reads of WhSBV persistently infected GSB are available in the Sequence Read Archive (SRA) under SRR32424572, and RNAseq data have been deposited at ArrayExpress under E-MTAB-14894.

ACKNOWLEGEMENTS

The investigations were supported by a Friedrich-Loeffler-Institut internal PhD program, grant number FLI-IVD-XX-2021-83, granted to F.P.

We gratefully acknowledge the assistance of Fermin Georgio Lorenzen-Schmidt, Mathias Lenk from the Collection of Cell Lines in Veterinary Medicine (CCLV), and the contributions of Robin Brandt, and Kristin Vorpahl.

CONFLICT OF INTEREST

The authors declare no conflicts of interest. The funders had no role in study design, data collection, analysis, interpretation, manuscript writing, or decision to publish the findings.

REFERENCES

Amarasinghe, Gaya K.; Ayllón, María A.; Bào, Yīmíng; Basler, Christopher F.; Bavari, Sina; Blasdell, Kim R. et al. (2019): Taxonomy of the order Mononegavirales: update 2019. In *Archives of virology* 164 (7), pp. 1967–1980. DOI: 10.1007/s00705-019-04247-4.

Banerjee, A. K.; Barik, S.; De, B. P. (1991): Gene expression of nonsegmented negative strand RNA viruses. In *Pharmacology & therapeutics* 51 (1), pp. 47–70. DOI: 10.1016/0163-7258(91)90041-j.

Barr, John N.; Whelan, Sean P. J.; Wertz, Gail W. (2002): Transcriptional control of the RNA-dependent RNA polymerase of vesicular stomatitis virus. In *Biochimica et biophysica acta* 1577 (2), pp. 337–353. DOI: 10.1016/S0167-4781(02)00462-1.

Briese, T.; La Torre, J. C. de; Lewis, A.; Ludwig, H.; Lipkin, W. I. (1992): Borna disease virus, a negative-strand RNA virus, transcribes in the nucleus of infected cells. In *Proceedings of the National Academy of Sciences of the United States of America* 89 (23), pp. 11486–11489. DOI: 10.1073/pnas.89.23.11486.

Briese, T.; Schneemann, A.; Lewis, A. J.; Park, Y. S.; Kim, S.; Ludwig, H.; Lipkin, W. I. (1994): Genomic organization of Borna disease virus. In *Proceedings of the National Academy of Sciences of the United States of America* 91 (10), pp. 4362–4366. DOI: 10.1073/pnas.91.10.4362.

Chang, Ming-Xian; Zou, Jun; Nie, Pin; Huang, Bei; Yu, Zhanglong; Collet, Bertrand; Secombes, Chris J. (2013): Intracellular interferons in fish: a unique means to combat viral infection. In *PLoS Pathogens* 9 (11), e1003736. DOI: 10.1371/journal.ppat.1003736.

Costa, Vincenzo A.; Mifsud, Jonathon C. O.; Gilligan, Dean; Williamson, Jane E.; Holmes, Edward C.; Geoghegan, Jemma L. (2021): Metagenomic sequencing reveals a lack of virus exchange between native and invasive freshwater fish across the Murray-Darling Basin, Australia. In *Virus evolution* 7 (1), veab034. DOI: 10.1093/ve/veab034.

Cox, Jürgen; Mann, Matthias (2008): MaxQuant enables high peptide identification rates, individualized p.p.b.-range mass accuracies and proteome-wide protein quantification. In *Nature biotechnology* 26 (12), pp. 1367–1372. DOI: 10.1038/nbt.1511.

Cubitt, B.; Oldstone, C.; Valcarcel, J.; La Carlos de Torre, J. (1994): RNA splicing contributes to the generation of mature mRNAs of Borna disease virus, a non-segmented negative strand RNA virus. In *Virus research* 34 (1), pp. 69–79. DOI: 10.1016/0168-1702(94)90120-1.

Cubitt, Beatrice; Ly, Calvin; La Torre, Juan Carlos de (2001): Identification and characterization of a new intron in Borna disease virus. In *The Journal of general virology* 82 (Pt 3), pp. 641–646. DOI: 10.1099/0022-1317-82-3-641.

Del Ortega-Villaizan, Maria Mar; Chico, Veronica; Perez, Luis (2022): Fish Innate Immune Response to Viral Infection-An Overview of Five Major Antiviral Genes. In *Viruses* 14 (7). DOI: 10.3390/v14071546.

Eshak, Mirette I. Y.; Rubbenstroth, Dennis; Beer, Martin; Pfaff, Florian (2023): Diving deep into fish bornaviruses: Uncovering hidden diversity and transcriptional strategies through comprehensive data mining. In *Virus evolution* 9 (2), vead062. DOI: 10.1093/ve/vead062.

Ewels, Philip A.; Peltzer, Alexander; Fillinger, Sven; Patel, Harshil; Alneberg, Johannes; Wilm, Andreas et al. (2020): The nf-core framework for community-curated bioinformatics pipelines. In *Nature biotechnology* 38 (3), pp. 276–278. DOI: 10.1038/s41587-020-0439-x.

Feng, Hui; Zhang, Yi-Bing; Zhang, Qi-Min; Li, Zhi; Zhang, Qi-Ya; Gui, Jian-Fang (2015): Zebrafish IRF1 regulates IFN antiviral response through binding to IFNφ1 and IFNφ3 promoters downstream of MyD88 signaling. In *Journal of immunology (Baltimore, Md. : 1950)* 194 (3), pp. 1225–1238. DOI: 10.4049/jimmunol.1402415.

Habjan, Matthias; Andersson, Ida; Klingström, Jonas; Schümann, Michael; Martin, Arnold; Zimmermann, Petra et al. (2008): Processing of genome 5' termini as a strategy of negative-strand RNA viruses to avoid RIG-I-dependent interferon induction. In *PloS one* 3 (4), e2032. DOI: 10.1371/journal.pone.0002032.

Hamming, Ole Jensen; Lutfalla, Georges; Levraud, Jean-Pierre; Hartmann, Rune (2011): Crystal structure of Zebrafish interferons I and II reveals conservation of type I interferon structure in vertebrates. In *Journal of virology* 85 (16), pp. 8181–8187. DOI: 10.1128/JVI.00521-11.

Herzog, S.; Rott, R. (1980): Replication of Borna disease virus in cell cultures. In *Medical microbiology and immunology* 168 (3), pp. 153–158. DOI: 10.1007/BF02122849.

Hoffmann, Bernd; Tappe, Dennis; Höper, Dirk; Herden, Christiane; Boldt, Annemarie; Mawrin, Christian et al. (2015): A Variegated Squirrel Bornavirus Associated with Fatal

Human Encephalitis. In *The New England journal of medicine* 373 (2), pp. 154–162. DOI: 10.1056/nejmoa1415627.

Huang, Zhilin; Chen, Song; Liu, Jiachen; Xiao, Jun; Yan, Jun; Feng, Hao (2015): IFNa of black carp is an antiviral cytokine modified with N-linked glycosylation. In *Fish & shellfish immunology* 46 (2), pp. 477–485. DOI: 10.1016/j.fsi.2015.07.020.

Hyndman, Timothy H.; Shilton, Catherine M.; Stenglein, Mark D.; Wellehan, James F. X. (2018): Divergent bornaviruses from Australian carpet pythons with neurological disease date the origin of extant Bornaviridae prior to the end-Cretaceous extinction. In *PLoS Pathogens* 14 (2). DOI: 10.1371/journal.ppat.1006881.

Kane, Melissa; Zang, Trinity M.; Rihn, Suzannah J.; Zhang, Fengwen; Kueck, Tonya; Alim, Mudathir et al. (2016): Identification of Interferon-Stimulated Genes with Antiretroviral Activity. In *Cell host & microbe* 20 (3), pp. 392–405. DOI: 10.1016/j.chom.2016.08.005.

Kuhn, Jens H.; Dürrwald, Ralf; Bào, Yīmíng; Briese, Thomas; Carbone, Kathryn; Clawson, Anna N. et al. (2015): Taxonomic reorganization of the family Bornaviridae. In *Archives of virology* 160 (2), pp. 621–632. DOI: 10.1007/s00705-014-2276-z.

Liang, Hong-Ru; Li, Yong-Gang; Zeng, Wei-Wei; Wang, Ying-Ying; Wang, Qing; Wu, Shu-Qin (2014): Pathogenicity and tissue distribution of grass carp reovirus after intraperitoneal administration. In *Virology journal* 11, p. 178. DOI: 10.1186/1743-422X-11-178.

Ma, Jie; Wang, Weiming; Zeng, Lingbing; Fan, Yuding; Xu, Jin; Zhou, Yong (2011): Inhibition of the replication of grass carp reovirus in CIK cells with plasmid-transcribed shRNAs. In *Journal of virological methods* 175 (2), pp. 182–187. DOI: 10.1016/j.jviromet.2011.05.008.

McLaughlin, Sara Koenig; Olsen, Sarah Naomi; Dake, Benjamin; Raedt, Thomas de; Lim, Elgene; Bronson, Roderick Terry et al. (2013): The RasGAP gene, RASAL2, is a tumor and metastasis suppressor. In *Cancer cell* 24 (3), pp. 365–378. DOI: 10.1016/j.ccr.2013.08.004.

Meyer, Bjoern; Ly, Hinh (2016): Inhibition of Innate Immune Responses Is Key to Pathogenesis by Arenaviruses. In *Journal of virology* 90 (8), pp. 3810–3818. DOI: 10.1128/JVI.03049-15.

Negishi, Hideo; Taniguchi, Tadatsugu; Yanai, Hideyuki (2018): The Interferon (IFN) Class of Cytokines and the IFN Regulatory Factor (IRF) Transcription Factor Family. In *Cold Spring Harbor perspectives in biology* 10 (11). DOI: 10.1101/cshperspect.a028423.

Nehyba, Jirí; Hrdlicková, Radmila; Bose, Henry R. (2009): Dynamic evolution of immune system regulators: the history of the interferon regulatory factor family. In *Molecular biology and evolution* 26 (11), pp. 2539–2550. DOI: 10.1093/molbev/msp167.

Niller, Hans Helmut; Angstwurm, Klemens; Rubbenstroth, Dennis; Schlottau, Kore; Ebinger, Arnt; Giese, Sebastian et al. (2020): Zoonotic spillover infections with Borna disease virus 1 leading to fatal human encephalitis, 1999-2019: an epidemiological investigation. In *The Lancet. Infectious diseases* 20 (4), pp. 467–477. DOI: 10.1016/s1473-3099(19)30546-8.

Nowotny, N.; Kolodziejek, J.; Jehle, C. O.; Suchy, A.; Staeheli, P.; Schwemmle, M. (2000): Isolation and characterization of a new subtype of Borna disease virus. In *Journal of virology* 74 (12), pp. 5655–5658. DOI: 10.1128/jvi.74.12.5655-5658.2000.

Pham, Phuc H.; Leacy, Alexander; Deng, Li; Nagy, Éva; Susta, Leonardo (2020): Isolation of Ontario aquatic bird bornavirus 1 and characterization of its replication in immortalized avian cell lines. In *Virology journal* 17 (1), p. 16. DOI: 10.1186/s12985-020-1286-6.

Poenisch, Marion; Wille, Sandra; Staeheli, Peter; Schneider, Urs (2008): Polymerase read-through at the first transcription termination site contributes to regulation of borna disease virus gene expression. In *Journal of virology* 82 (19), pp. 9537–9545. DOI: 10.1128/jvi.00639-08.

Qi, Zhitao; Nie, Pin; Secombes, Chris J.; Zou, Jun (2010): Intron-containing type I and type III IFN coexist in amphibians: refuting the concept that a retroposition event gave rise to type I IFNs. In *Journal of immunology (Baltimore, Md. : 1950)* 184 (9), pp. 5038–5046. DOI: 10.4049/jimmunol.0903374.

Rappsilber, Juri; Mann, Matthias; Ishihama, Yasushi (2007): Protocol for micro-purification, enrichment, pre-fractionation and storage of peptides for proteomics using StageTips. In *Nature protocols* 2 (8), pp. 1896–1906. DOI: 10.1038/nprot.2007.261.

Reuter, Antje; Ackermann, Andreas; Kothlow, Sonja; Rinder, Monika; Kaspers, Bernd; Staeheli, Peter (2010): Avian bornaviruses escape recognition by the innate immune system. In *Viruses* 2 (4), pp. 927–938. DOI: 10.3390/v2040927.

Rinder, Monika; Ackermann, Andreas; Kempf, Hermann; Kaspers, Bernd; Korbel, Rüdiger; Staeheli, Peter (2009): Broad tissue and cell tropism of avian bornavirus in parrots with proventricular dilatation disease. In *Journal of virology* 83 (11), pp. 5401–5407. DOI: 10.1128/JVI.00133-09.

Rubbenstroth, D.; Rinder, M.; Kaspers, B.; Staeheli, P. (2012): Efficient isolation of avian bornaviruses (ABV) from naturally infected psittacine birds and identification of a new ABV genotype from a salmon-crested cockatoo (Cacatua moluccensis). In *Veterinary microbiology* 161 (1-2), pp. 36–42. DOI: 10.1016/j.vetmic.2012.07.004.

Rubbenstroth, Dennis; Briese, Thomas; Dürrwald, Ralf; Horie 堀江真行, Masayuki; Hyndman, Timothy H.; Kuhn, Jens H. et al. (2021): ICTV Virus Taxonomy Profile: Bornaviridae. In *The Journal of general virology* 102 (7). DOI: 10.1099/jgv.0.001613.

Rubbenstroth, Dennis; Rinder, Monika; Stein, Malte; Höper, Dirk; Kaspers, Bernd; Brosinski, Katrin et al. (2013): Avian bornaviruses are widely distributed in canary birds (Serinus canaria f. domestica). In *Veterinary microbiology* 165 (3-4), pp. 287–295. DOI: 10.1016/j.vetmic.2013.03.024.

Rubbenstroth, Dennis; Schmidt, Volker; Rinder, Monika; Legler, Marko; Corman, Victor Max; Staeheli, Peter (2014): Discovery of a new avian bornavirus genotype in estrildid finches (Estrildidae) in Germany. In *Veterinary microbiology* 168 (2-4), pp. 318–323. DOI: 10.1016/j.vetmic.2013.11.032.

Schlottau, Kore; Nobach, Daniel; Herden, Christiane; Finke, Stefan; Beer, Martin; Hoffmann, Donata (2020): First isolation, in-vivo and genomic characterization of zoonotic variegated squirrel Bornavirus 1 (VSBV-1) isolates. In *Emerging microbes & infections* 9 (1), pp. 2474–2484. DOI: 10.1080/22221751.2020.1847604.

Schneemann, A.; Schneider, P. A.; Kim, S.; Lipkin, W. I. (1994): Identification of signal sequences that control transcription of borna disease virus, a nonsegmented, negative-strand RNA virus. In *Journal of virology* 68 (10), pp. 6514–6522. DOI: 10.1128/JVI.68.10.6514-6522.1994.

Schneemann, A.; Schneider, P. A.; Lamb, R. A.; Lipkin, W. I. (1995): The remarkable coding strategy of borna disease virus: a new member of the nonsegmented negative strand RNA viruses. In *Virology* 210 (1), pp. 1–8. DOI: 10.1006/viro.1995.1311.

Schneider, P. A.; Schneemann, A.; Lipkin, W. I. (1994): RNA splicing in Borna disease virus, a nonsegmented, negative-strand RNA virus. In *Journal of virology* 68 (8), pp. 5007–5012. DOI: 10.1128/JVI.68.8.5007-5012.1994.

Shi, Mang; Lin, Xian-Dan; Chen, Xiao; Tian, Jun-Hua; Chen, Liang-Jun; Li, Kun et al. (2018): The evolutionary history of vertebrate RNA viruses. In *Nature* 556 (7700), pp. 197–202. DOI: 10.1038/s41586-018-0012-7.

Song, Wuqi; Kao, Wenping; Zhai, Aixia; Qian, Jun; Li, Yujun; Zhang, Qingmeng et al. (2013): Borna disease virus nucleoprotein inhibits type I interferon induction through the interferon regulatory factor 7 pathway. In *Biochemical and biophysical research communications* 438 (4), pp. 619–623. DOI: 10.1016/j.bbrc.2013.08.006.

Tomonaga, K.; Kobayashi, T.; Lee, B. J.; Watanabe, M.; Kamitani, W.; Ikuta, K. (2000): Identification of alternative splicing and negative splicing activity of a nonsegmented negative-strand RNA virus, Borna disease virus. In *Proceedings of the National Academy of Sciences of the United States of America* 97 (23), pp. 12788–12793. DOI: 10.1073/pnas.97.23.12788.

Tomonaga, Keizo; Kobayashi, Takeshi; Ikuta, Kazuyoshi (2002): Molecular and cellular biology of Borna disease virus infection. In *Microbes and infection* 4 (4), pp. 491–500. DOI: 10.1016/s1286-4579(02)01564-2.

Unterstab, Gunhild; Ludwig, Stephan; Anton, Aline; Planz, Oliver; Dauber, Bianca; Krappmann, Daniel et al. (2005): Viral targeting of the interferon-{beta}-inducing Traf family member-associated NF-{kappa}B activator (TANK)-binding kinase-1. In *Proceedings of the National Academy of Sciences of the United States of America* 102 (38), pp. 13640–13645. DOI: 10.1073/pnas.0502883102.

Wignall-Fleming, Elizabeth B.; Hughes, David J.; Vattipally, Sreenu; Modha, Sejal; Goodbourn, Steve; Davison, Andrew J.; Randall, Richard E. (2019): Analysis of Paramyxovirus Transcription and Replication by High-Throughput Sequencing. In *Journal of virology* 93 (17). DOI: 10.1128/JVI.00571-19.

Xue, Shuqun; Lin, Jiawen; Han, Yue; Han, Ying (2021): Ammonia stress–induced apoptosis by p53–BAX/BCL-2 signal pathway in hepatopancreas of common carp (Cyprinus carpio). In *Aquacult Int* 29 (4), pp. 1895–1907. DOI: 10.1007/s10499-021-00724-3.

Yang, Yuru; Wang, Yingying; Wang, Qing; Zeng, Weiwei; Li, Yingying; Yin, Jiyuan et al. (2021): Establishment of a cell line from swim bladder of the Grass carp (Ctenopharyngodon idellus) for propagation of Grass Carp Reovirus Genotype II. In *Microbial pathogenesis* 151, p. 104739. DOI: 10.1016/j.micpath.2021.104739.

Yu, Dong-Shan; Weng, Tian-Hao; Wu, Xiao-Xin; Wang, Frederick X. C.; Lu, Xiang-Yun; Wu, Hai-Bo et al. (2017): The lifecycle of the Ebola virus in host cells. In *Oncotarget* 8 (33), pp. 55750–55759. DOI: 10.18632/oncotarget.18498.

FIGURES

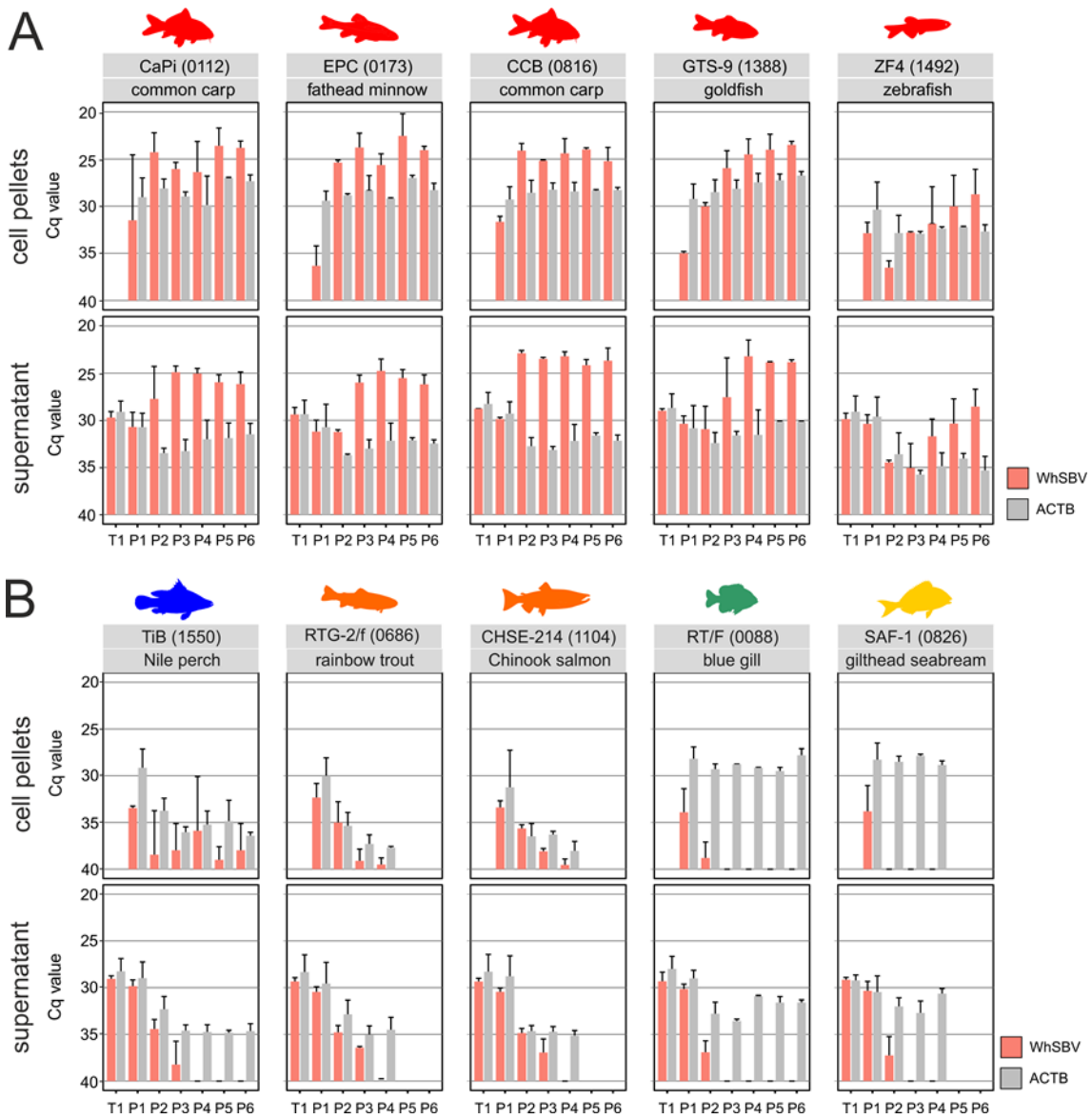

Figure 1: WhSBV RNA levels over successive passages in different fish cell lines. Different fish cell lines were inoculated with WhSBV. The cells were then passaged for 4-6 times by splitting. (**A**) Cell lines from the taxonomic order of Cypriniformes (red); (**B**) Cell lines from the taxonomic orders of Chichliformes (blue), Salmoniformes (orange), Centrarchiformes (green) and Spariformes (yellow). RNA levels of viral glycoprotein (WhSBV; red bars) and cellular beta actin (ACTB; grey bars) genes were detected by specific RT-qPCR in cell pellets (top row) and cell culture supernatants (bottom row) from each passage. Results are presented as the arithmetic mean (± standard deviation) of the cycle of quantification (Cq) values of two independent experiments.

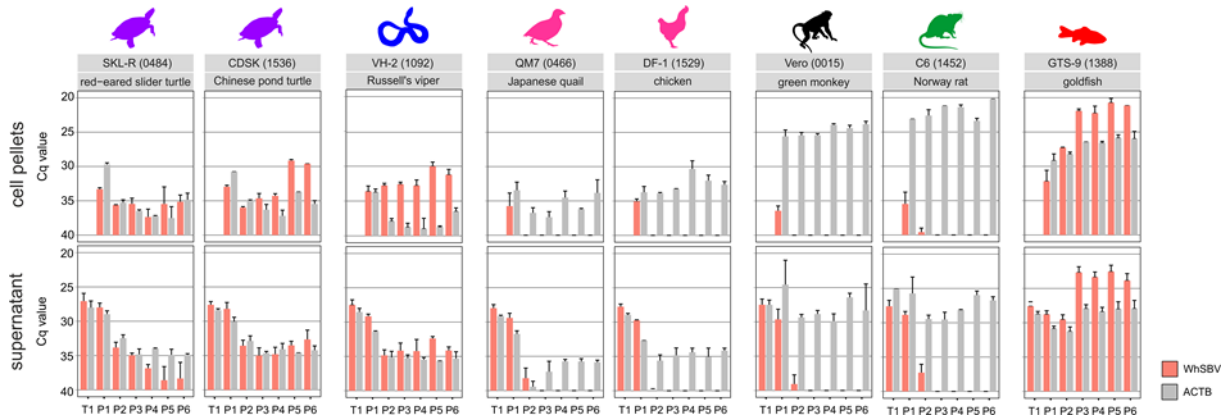

Figure 2: WhSBV RNA levels over successive passages in different non-fish cell lines. Different cell lines from the taxonomic orders of Testudines (purple), Squamata (blue), Galliformes (pink), Primates (black), and Rodentia (green) were inoculated with WhSBV and subsequently passaged for 6 times by splitting of the cells. The cypriniform fish cell line GTS-9 (red) was used as a positive control to validate the infection experiment. RNA levels of viral glycoprotein (WhSBV; red bars) and cellular beta actin (ACTB; grey bars) genes were detected by specific RT-qPCR in cell pellets (top row) and cell culture supernatants (bottom row) from each passage. Results are presented as the arithmetic mean (± standard deviation) of the cycle of quantification (Cq) values of two independent experiments.

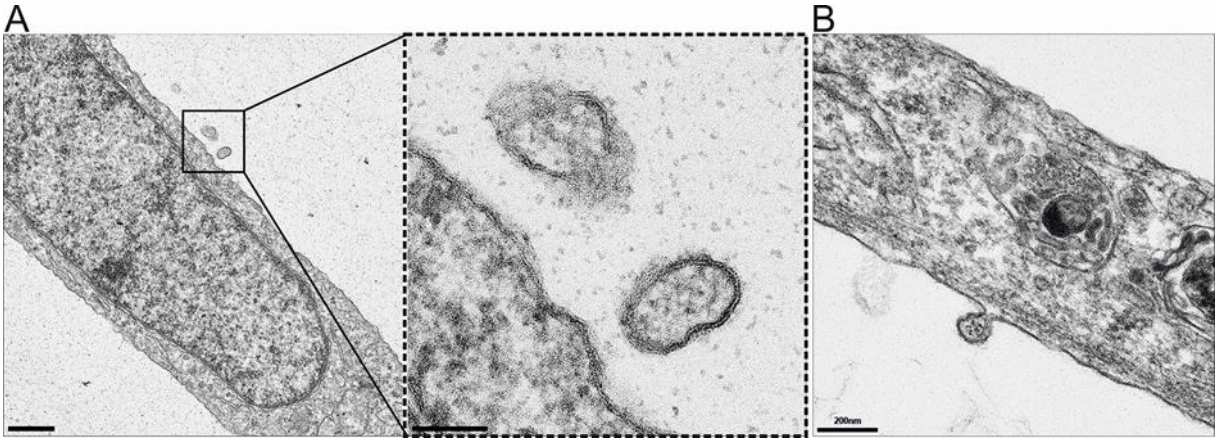

Figure 3: Detection of bornavirid-like particles by electron microscopy. (**A**) Bornavirid-like particles detected in the experimentally infected ZF4 cell line. The WhSBV virions are spherical to pleomorphic in shape, with a diameter of approximately 150-180 nm. (**B**) A potential WhSBV virion budding from the persistently WhSBV-infected GSB cell line.

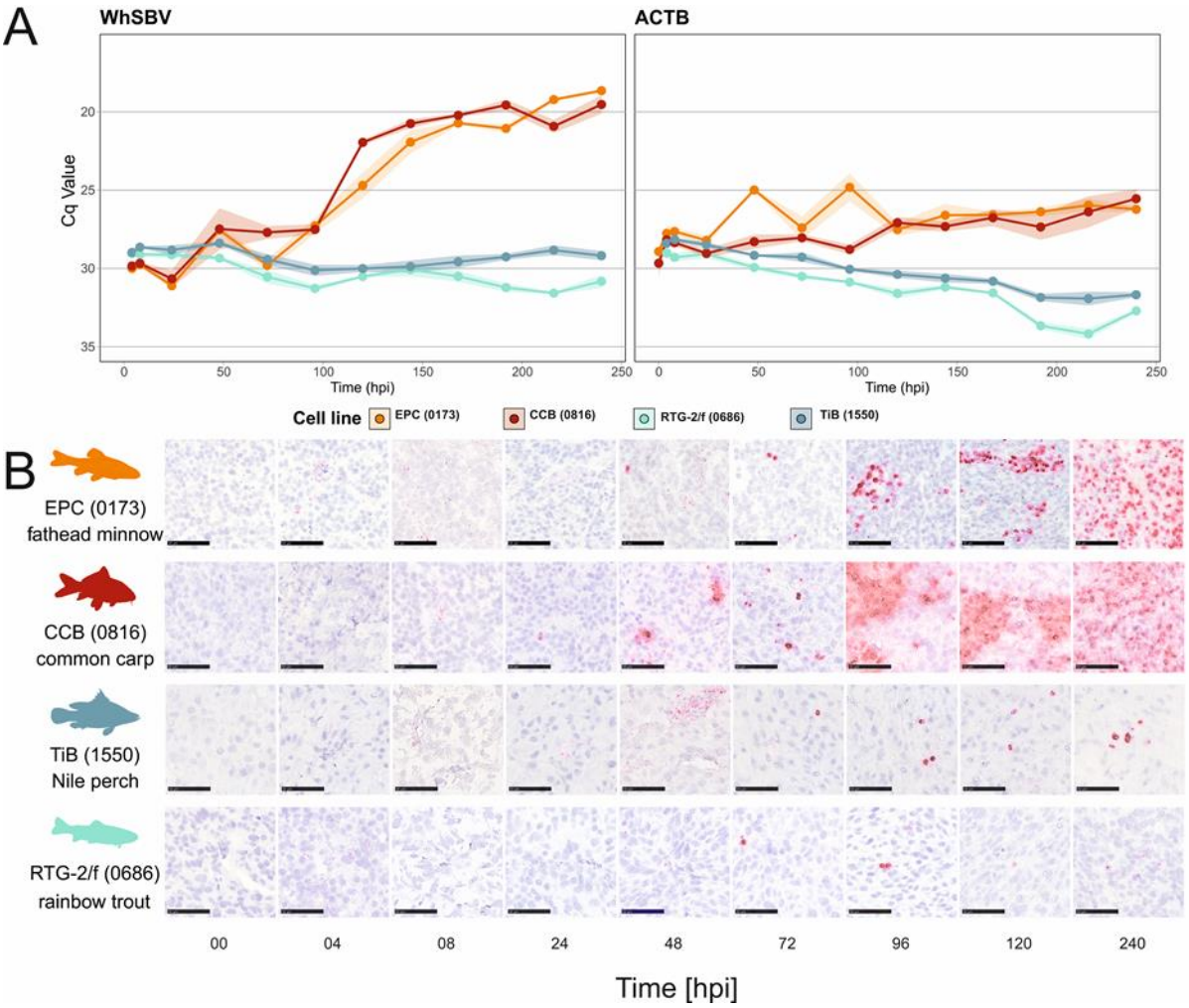

Figure 4: Detection of viral RNA by RT-qPCR and RNA *in situ* hybridisation. (**A**) RNA levels of the viral glycoprotein (WhSBV) and cellular beta actin (ACTB) genes were detected by reverse transcription quantitative PCR (RT-qPCR) and are presented as cycle of quantification (Cq) values for RNA extracted from cell pellets of EPC (orange), CCB (red), RTG-2/f (greenish-blue) and TiB (blue-grey) at different hours post inoculation (hpi). Results are presented as arithmetic means (± standard deviation) of three replicates. (**B**) Detection of viral RNA by RNA *in situ* hybridisation in formalin-fixed cell pellets from WhSBV-inoculated cypriniform (CCB, EPC) and non-cypriniform (TiB, RTG-2/f) cell lines. One representative image is shown for each cell line and time point. The black scale bar represents 50 µm.

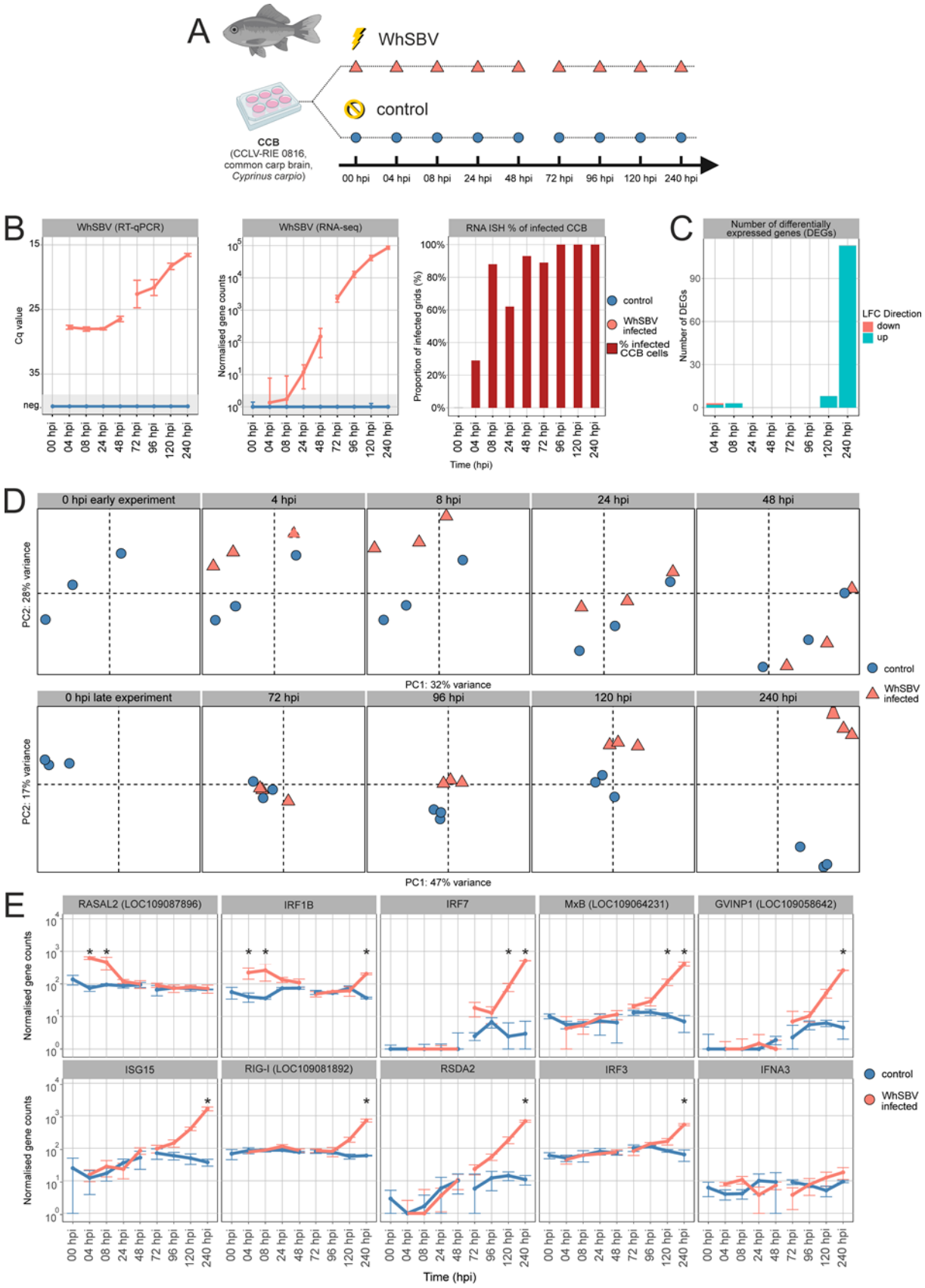

Figure 5: Cellular response to early and late WhSBV infection in the cypriniform brain cells CCB. (**A**) CCB cells were experimentally WhSBV-infected (orange triangles) and mock-

infected (blue dots) in two consecutive experiments, covering early (0, 4, 8, 24, and 48 hours post infection (hpi)) and late (0, 72, 96, 120, and 240 hpi) infection stages, respectively. (**B**) Viral RNA was detected by reverse transcription quantitative PCR (RT-qPCR; left panel) and RNA sequencing (RNAseq; middle panel). The RT-qPCR targeted the viral glycoprotein and is presented as cycle of quantification values (Cq), while RNAseq quantified sequence reads corresponding to the WhSBV genome and is presented as normalised gene counts. Arithmetic means (± standard deviation, SD) of three replicate wells are shown for Cq values and normalised gene counts. WhSBV-specific RNA *in situ* hybridisation (RNA ISH) data from a separate experiment are shown for comparison (right panel; see Supplementary Figure S4). (**C**) Differentially expressed genes (DEGs) with an absolute log-fold change (LFC) of > 1 and an adjusted *p-value* < 0.05 were derived from the RNAseq data using the DESeq2 package (v1.40), and their number and LFC direction are shown for each time point. (**D**) Principal component analysis (PCA) was performed on the RNAseq gene expression data using R (v4.3.1). Orange triangles and blue dots represent replicates of WhSBV-infected and mock-infected CCB cells, respectively. (**E**) Trends in transcript levels of selected genes known to be key antiviral genes in the early innate immune response to viral infection in fish. These genes include RASAL2 (RAS GTPase-activating protein 2-like [LOC109087896]), IRF1B (interferon regulatory factor 1), IRF7 (interferon regulatory factor 7), IRF3 (interferon regulatory factor 3), MxB (interferon-induced GTP-binding protein MxB-like), GVINP1 (interferon-induced very large GTPase 1-like [LOC109058642]), ISG15 (interferon-stimulated gene 15), RIG-I (antiviral innate immune response receptor RIG-I [LOC109081892]), RSDA2 (viperin, radical S-adenosyl methionine domain containing 2) and IFNA3 (interferon-alpha 3). Asterisks indicate time points with significantly differentially gene expression as compared to uninfected controls. The complete list of DEGs can be found in Supplementary Table S4. Results are presented as the arithmetic/geometric mean (± standard deviation) of three replicate wells.

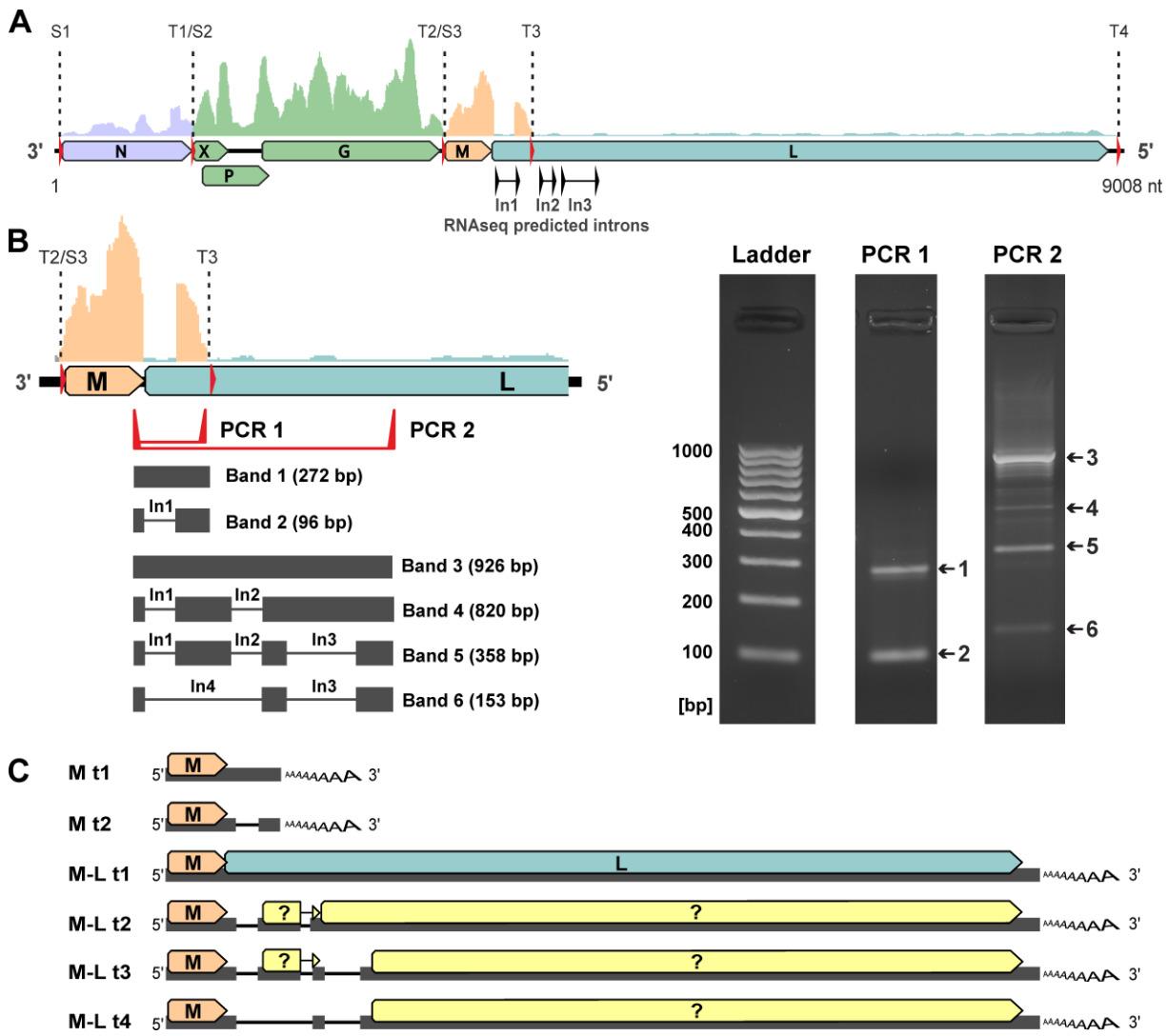

Figure 6: Detection of spliced WhSBV RNA in persistently WhSBV-infected CiSB cells. (**A**) Raw reads from the metagenomic RNA sequencing of the persistently WhSBV-infected CiSB cell line dataset were mapped to the corresponding WhSBV genome and the resulting coverage was plotted. Mapping was performed using the generic Geneious Prime mapper with medium sensitivity settings (options: find structural variants, short insertions, and deletions of any size). In the schematic WhSBV genome, open reading frames (ORFs) are shown as arrows and transcription start sites (S1-S3) and termination sites (T1-4) are shown as dashed lines. ORFs that are likely to be located on the same RNA transcript are shown in the same colour. Three splicing events (introns In1-3) were detected within the L ORF region using the Geneious Prime mapper. (**B**) RNA was extracted from the persistently WhSBV-infected CiSB cell line and cDNA was synthesised using oligo-dT primers. A PCR was performed using this cDNA and primers targeting the predicted M and L splice sites (PCR 1 and 2). The PCR products were run on a 2% agarose gel (right panel). Bands 1-6 were excised, purified and sequenced by Sanger sequencing. The sequences were mapped back to the respective WhSBV genome in order to confirm the predicted introns In1-4 (black lines).

(**C**) Alternative transcripts of WhSBV were inferred from the detected splice sites and transcription start and termination sites. The schematic shows six alternative transcripts, designated as M transcripts 1-2 (M t1-t2) or M-L transcripts 1-4 (t1-t4). Arrows indicate possible ORFs.

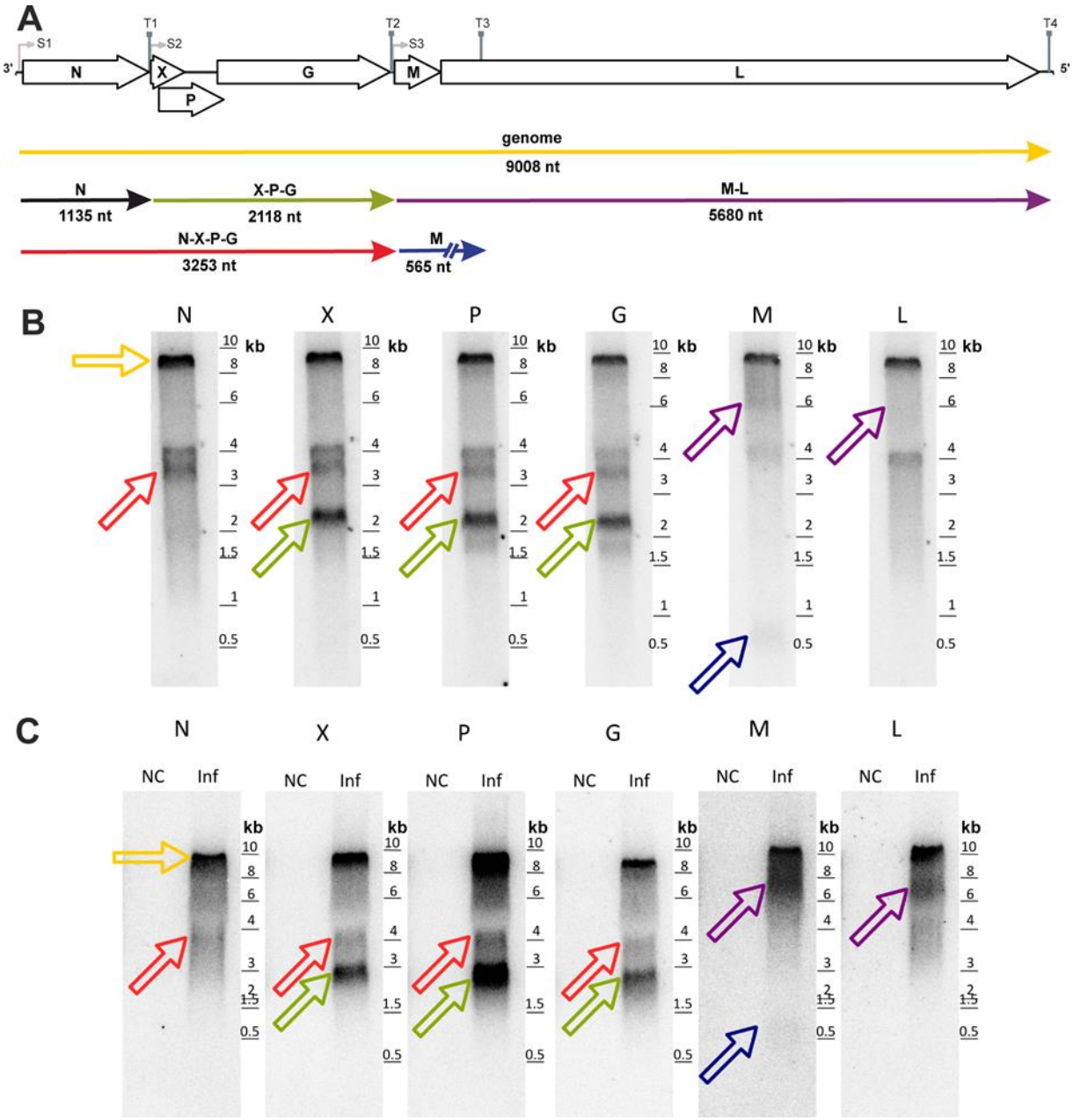

Figure 7: Detection of multicistronic WhSBV RNA in persistently WhSBV-infected and WhSBV-inoculated cells. WhSBV RNA transcripts were detected by Northern blot using ^{32}P-CTP-labelled probes specific for WhSBV genes (arrows) encoding for the nucleoprotein (N), accessory protein (X), phosphoprotein (P), matrix protein (M), glycoprotein (G), and the

large protein (L). For reference, a schematic representation of the WhSBV genome, along with open reading frames (arrows) and possible RNA molecules (coloured lines) is shown in **(A).** Total RNA from the persistently WhSBV-infected GSB cell line **(B)** and WhSBV-inoculated (Inf) EPC cells compared to non-WhSBV-inoculated (NC) EPC cells **(C)**, was used for the Northern blot. Probes that detected RNA species of the same size were interpreted as corresponding to the same RNA molecule. The coloured arrows in **(B)** and **(C)** correspond to the respective WhSBV RNA molecules in the schematic. A ladder is provided in kilobase pairs (kb).

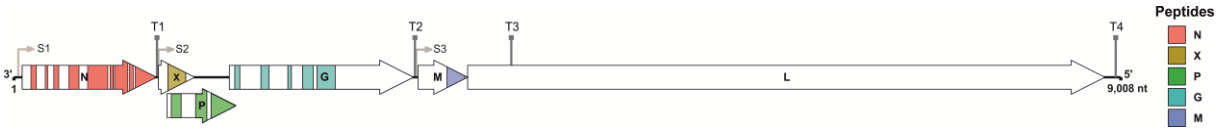

Figure 8: Detection of WhSBV viral peptides in persistently WhSBV-infected GSB cells. High resolution mass spectrometry was performed on protein extracts from the persistently WhSBV-infected GSB cells. Mass spectrometry raw files were processed with MaxQuant (version 2.4.13.0) (Cox and Mann 2008) using a custom virus database (6 entries) and the *C. idella* database (C_idella_female_genemodels.v1; 32,811 entries) with default settings. The figure shows a schematic representation of the complete viral genome, with open reading frames (ORF) indicated by as arrows and transcription start (S1-S3) and termination sites (T1-4). Areas corresponding to detected peptides are colour coded for each associated ORF. No peptides matching the L protein or fused peptides were detected.